

Estimating Density Models with Truncation Boundaries using Score Matching

Song Liu

song.liu@bristol.ac.uk

University of Bristol

Takafumi Kanamori

kanamori@c.titech.ac.jp

Tokyo Institute of Technology; RIKEN AIP

Daniel J. Williams

daniel.williams@bristol.ac.uk

University of Bristol

Abstract

Truncated densities are probability density functions defined on truncated domains. They share the same parametric form with their non-truncated counterparts up to a normalizing constant. Since the computation of their normalizing constants is usually infeasible, Maximum Likelihood Estimation cannot be easily applied to estimate truncated density models. Score Matching (SM) is a powerful tool for fitting parameters using only unnormalized models. However, it cannot be directly applied here as boundary conditions used to derive a tractable SM objective are not satisfied by truncated densities. In this paper, we study parameter estimation for truncated probability densities using SM. The estimator minimizes a weighted Fisher divergence. The weight function is simply the shortest distance from the data point to the boundary of the domain. We show this choice of weight function naturally arises from minimizing the Stein discrepancy as well as upperbounding the finite-sample estimation error. The usefulness of our method is demonstrated by numerical experiments and a study on Chicago crime dataset. We also show that the proposed density estimation can correct the outlier-trimming bias caused by aggressive outlier detection methods.

1 Introduction

In many applications, we cannot observe the “full picture” of a problem. Instead, our window of observation is limited, so we can only observe a truncated dataset. For example, a police

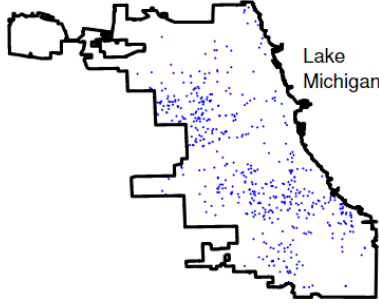


Figure 1: Boundary of Chicago, where blue dots are locations of homicides in 2008.

department can only monitor crimes within their city’s boundary, despite that crimes do not automatically stop at an artificial border. Similarly, geolocation tracking data can only be observed up to the coverage of mobile signal. Thus these datasets are skewed representations of actual activities. In many cases, truncation boundaries can be very complex. For example, the boundary of the city of Chicago is a complex polygon (see Figure 1) which cannot be easily approximated by a bounding box or circle.

The key challenge of estimating parameters in truncated densities is that the normalizing constant is not computationally tractable. The normalizing constant ensures that the integration of a density function equals to one over its input domain. As the normalization takes place in a irregular bounded domain in \mathbb{R}^d , the integration does not have a closed form in general. This creates a computational issue since the classic Maximum Likelihood Estimation (MLE) requires the evaluation of such a normalizing constant.

Recent years have seen a new class of estimators, called Score Matching (SM) [Hyvärinen, 2005, 2007, Lyu, 2009] rise in popularity. They estimate parameters by minimizing the Fisher-Hyvärinen divergence [Lyu, 2009]. The divergence is defined using the difference between the gradients of log model density and log data density. The gradients are taken with respect to the *input variable*, so the normalizing constant is eliminated and is not involved in the estimation procedure. Thus SM is a natural candidate for estimating truncated density models.

The original SM does not work on truncated models. This is due to the regularity condition used to derive the tractable objective function is not satisfied. Hyvärinen and Yu et al. proposed *generalized SM* to handle the distributions on the positive orthant \mathbb{R}_+^d . In generalized SM, a weight function is introduced so that the boundary condition required for deriving the tractable objective function is satisfied. Promising results have been observed on high-dimensional non-negative graphical model structure estimation [Yu et al., 2019]. When the density is truncated in a dimension-wise manner with a lower and upper bound, this problem is known as a doubly truncated distribution estimation [Turnbull, 1976, Moreira and de Uña-Álvarez, 2012]. Though some works have tackled the problem of estimating truncated multivariate Gaussian densities [Daskalakis et al., 2018, 2019], little work has been done for estimating a wide range of density models with complicated truncation domains.

In this paper, we proposed a novel estimator for truncated density models using generalized

SM. Our choice of the weight function is the distance from the data point to the truncation boundary. Such a choice naturally arises from minimizing a Stein Discrepancy and lowering the finite sample estimation error bound. We also show that this weight function can be easily computed for many complicated domains.

The usefulness of our method is demonstrated by numerical experiments and an application on the Chicago crime dataset. Finally we apply this estimator to correct the outlier trimming bias caused by One-class Support Vector Machines.

2 Problem Formulation

Denote a probability density function over the domain $V \subset \mathbb{R}^d$ as $p_{\boldsymbol{\theta}}(\mathbf{x})$, $\mathbf{x} \in V$ with the parameter $\boldsymbol{\theta}$. Without loss of generality, we can write $p_{\boldsymbol{\theta}}(\mathbf{x}) := \bar{p}_{\boldsymbol{\theta}}(\mathbf{x})/Z_V(\boldsymbol{\theta})$, where $\bar{p}_{\boldsymbol{\theta}}$ is an unnormalized model and $Z_V(\boldsymbol{\theta})$ is the normalizing constant defined by $Z_V(\boldsymbol{\theta}) := \int_V \bar{p}_{\boldsymbol{\theta}}(\mathbf{x})d\mathbf{x}$ so that $p_{\boldsymbol{\theta}}(\mathbf{x})$ is integrated to 1 over its domain V . The domain $V \subset \mathbb{R}^d$ may be a complicated bounded domain e.g., a polytope. In such cases, $Z_V(\boldsymbol{\theta})$ may not have a closed form and cannot be easily evaluated. For example, let $\bar{p}_{\boldsymbol{\theta}}$ be a Gaussian mixture model restricted in a generic polygon, then $Z_V(\boldsymbol{\theta})$ does not have a closed form expression.

Our task is classic statistical model estimation: Suppose that V is given, we want to estimate the parameter $\boldsymbol{\theta}$ in $p_{\boldsymbol{\theta}}(\mathbf{x})$ using $X_q = \{\mathbf{x}_i\}_{i=1}^n$, which is a set of observed i.i.d. samples from a truncated data generating distribution Q with an unknown probability density function $q(\mathbf{x})$, $\mathbf{x} \in V$.

The challenge comes from the fact that we need to obtain the estimator of $\boldsymbol{\theta}$ using only the unnormalized density model $\bar{p}_{\boldsymbol{\theta}}(\mathbf{x})$: It is not straightforward to calculate $Z_V(\boldsymbol{\theta})$ for a complicated V . Therefore, MLE, which requires us evaluating the normalizing constant, cannot be performed easily. A popular tool for estimating unnormalized densities is Score Matching (SM) proposed by [Hyvärinen](#). We now introduce SM and its extension [[Yu et al., 2019](#)], then explain why it cannot be readily used for estimating complicated truncated densities.

Notation: The finite set $\{1, \dots, d\}$ for a positive integer d is denoted by $[d]$. Given a vector \mathbf{x} , let x_k denote the k -th element of \mathbf{x} . Let $\langle \cdot, \cdot \rangle$ be the standard inner product, and the Euclidean norm of the vector \mathbf{a} is denoted as $\|\mathbf{a}\| = \sqrt{\langle \mathbf{a}, \mathbf{a} \rangle}$. The ℓ^p -norm of \mathbf{x} is denoted by $\|\mathbf{x}\|_p$. Thus, $\|\mathbf{x}\| = \|\mathbf{x}\|_2$ holds. Let ∂_k for $k \in [d]$ be the partial differential operator $\frac{\partial}{\partial x_k}$ and $\nabla_{\mathbf{x}}$ be $(\partial_1, \dots, \partial_d)$ to the function $f(\mathbf{x})$ for $\mathbf{x} \in \mathbb{R}^d$. Similarly, the gradient operator with respect to the parameter $\boldsymbol{\theta} \in \Theta \subset \mathbb{R}^r$ of the statistical model $p_{\boldsymbol{\theta}}(\mathbf{x})$ is denoted by $\nabla_{\boldsymbol{\theta}} = (\frac{\partial}{\partial \theta_1}, \dots, \frac{\partial}{\partial \theta_r})$. $\mathbb{E}_q[f(\mathbf{x})]$ stands for the expectation of $f(\mathbf{x})$ with respect to the probability density $q(\mathbf{x})$. To reduce the clutter, we sometimes shorten $p_{\boldsymbol{\theta}}(\mathbf{x})$ and $q(\mathbf{x})$ as $p_{\boldsymbol{\theta}}$ and q wherever such abbreviations do not lead to confusion. In addition, the log-likelihood $\log p_{\boldsymbol{\theta}}(\mathbf{x})$ is expressed by $\ell_{\boldsymbol{\theta}}(\mathbf{x})$. $\|f\|_{L^2(Q)} := (\mathbb{E}_q[f(\mathbf{x})^2])^{1/2}$ where Q denotes a distribution with density function $q(\mathbf{x})$. Let $\mathbf{e}_i, i = 1, \dots, d$ be the unit vector along the i -th axis in \mathbb{R}^d , i.e., $\mathbf{e}_1 = (1, 0, \dots, 0)$, etc. We use \bar{V} to represent the closure of a bounded open set V .

3 Score Matching and Its Generalization

In this section, we introduce classic SM [Hyvärinen, 2005] and one of its variants [Yu et al., 2019].

Definition 1. *The Fisher-Hyvärinen (FH) divergence [Lyu, 2009] between q and $p_{\boldsymbol{\theta}}$ is defined as*

$$\text{FH}(q, p_{\boldsymbol{\theta}}) := \mathbb{E}_q[\|\nabla_{\mathbf{x}} \log p_{\boldsymbol{\theta}}(\mathbf{x}) - \nabla_{\mathbf{x}} \log q(\mathbf{x})\|^2].$$

Suppose $q(\mathbf{x}) > 0$ on \mathbb{R}^d . Then, the FH divergence is non-negative and it vanishes if and only if $p_{\boldsymbol{\theta}}(\mathbf{x}) = q(\mathbf{x})$ almost surely. When a density model $p_{\boldsymbol{\theta}}(\mathbf{x})$ is defined on $V = \mathbb{R}^d$, SM finds an estimate of $\boldsymbol{\theta}$ by minimizing $\text{FH}(q, p_{\boldsymbol{\theta}})$ over the parameter space $\boldsymbol{\theta} \in \Theta \subset \mathbb{R}^r$, i.e.,

$$\begin{aligned} \boldsymbol{\theta}_{\text{SM}} &:= \underset{\boldsymbol{\theta}}{\text{argmin}} \text{FH}(q, p_{\boldsymbol{\theta}}) \\ &= \underset{\boldsymbol{\theta}}{\text{argmin}} \mathbb{E}_q[\|\nabla_{\mathbf{x}} \log p_{\boldsymbol{\theta}}\|^2] - 2\mathbb{E}_q[\langle \nabla_{\mathbf{x}} \log p_{\boldsymbol{\theta}}, \nabla_{\mathbf{x}} \log q \rangle] + C, \end{aligned} \quad (1)$$

where C is a constant independent of $\boldsymbol{\theta}$. The key advantage of SM is that the normalizing constant $Z_V(\boldsymbol{\theta})$ is not required when evaluating (1) as $\nabla_{\mathbf{x}} \log p_{\boldsymbol{\theta}}(\mathbf{x}) = \nabla_{\mathbf{x}} \log \bar{p}_{\boldsymbol{\theta}}(\mathbf{x})$. Thus, SM is widely used for estimating “unnormalizable” statistical models.

Unfortunately, (1) is not tractable as we cannot directly evaluate the second term of (1) without access to $\nabla_{\mathbf{x}} \log q$. Using the integration by parts rule, however, we find that the equality,

$$\mathbb{E}_q[\langle \nabla_{\mathbf{x}} \log p_{\boldsymbol{\theta}}, \nabla_{\mathbf{x}} \log q \rangle] = - \sum_{k=1}^d \mathbb{E}_q[\partial_k^2 \log p_{\boldsymbol{\theta}}]$$

holds under the smoothness condition of $\log p_{\boldsymbol{\theta}}(\mathbf{x})$ and $\log q(\mathbf{x})$ w.r.t. \mathbf{x} and the boundary condition

$$\lim_{|x_k| \rightarrow \infty} q(\mathbf{x}) \partial_k \log p_{\boldsymbol{\theta}}(\mathbf{x}) = 0, \forall k \in [d]. \quad (2)$$

Many density functions defined on \mathbb{R}^d , such as multivariate Gaussian or Gaussian mixture, satisfy these conditions. See [Hyvärinen, 2005, 2007] for details. Thus, FH-divergence in (1) can be re-written as

$$\text{FH}(q, p_{\boldsymbol{\theta}}) = \mathbb{E}_q[\|\nabla_{\mathbf{x}} \log p_{\boldsymbol{\theta}}\|^2] + 2 \sum_{k=1}^d \mathbb{E}_q[\partial_k^2 \log p_{\boldsymbol{\theta}}] + C \quad (3)$$

where the objective only relies on q through the expectations which can be approximated by the empirical mean over the observed samples X_q .

When $p_{\boldsymbol{\theta}}(\mathbf{x})$ is defined on the *truncated* subset in \mathbb{R}^d such as the positive orthant \mathbb{R}_+^d , the boundary condition (2) required to apply the integration by parts rule no longer holds

in general. To estimate parameters of density functions on the *positive orthant*, [Hyvärinen \[2007\]](#), [Yu et al. \[2019\]](#) introduced generalized SM:

$$\begin{aligned}\boldsymbol{\theta}_{\text{GSM}} &:= \underset{\boldsymbol{\theta}}{\operatorname{argmin}} \operatorname{FH}_{\mathbf{g}}(q, p_{\boldsymbol{\theta}}), \\ \operatorname{FH}_{\mathbf{g}}(q, p_{\boldsymbol{\theta}}) &:= \mathbb{E}_q[\|\mathbf{g}^{1/2} \circ \nabla_{\mathbf{x}} \log p_{\boldsymbol{\theta}} - \mathbf{g}^{1/2} \circ \nabla_{\mathbf{x}} \log q\|^2], \\ &= \sum_{k=1}^d \mathbb{E}_q[g_k \cdot (\partial_k \log p_{\boldsymbol{\theta}})^2] - 2 \sum_{k=1}^d \mathbb{E}_q[g_k \cdot (\partial_k \log p_{\boldsymbol{\theta}})(\partial_k \log q)] + C,\end{aligned}\quad (4)$$

where $\mathbf{g}(\mathbf{x}) := (g_1(\mathbf{x}), \dots, g_d(\mathbf{x})) \in \mathbb{R}^d$ is a non-negative valued, continuously differentiable function with $\mathbf{g}(\mathbf{0}) = \mathbf{0}$, $\mathbf{g}^{1/2}$ is the element-wise square root operation applied on \mathbf{g} and \circ is the element-wise product. Examples of \mathbf{g} include $g_k(\mathbf{x}) = x_k$ or $g_k(\mathbf{x}) = \max(x_k, 1), \forall k \in [d]$ given $\mathbf{x} \in \mathbb{R}_+^d$.

The following Lemma can be used to derive the tractable objective function from (4).

Lemma 1. *Suppose that $\log q(\mathbf{x})$ and $\mathbf{g}(\mathbf{x})$ are continuously differentiable and that $\log p_{\boldsymbol{\theta}}(\mathbf{x})$ is twice continuously differentiable with respect to \mathbf{x} on \mathbb{R}_+^d . Furthermore, we assume the boundary condition, $\lim_{|x_k| \rightarrow 0+, |x_k| \rightarrow \infty} g_k(\mathbf{x})q(\mathbf{x})\partial_k \log p_{\boldsymbol{\theta}}(\mathbf{x}) = 0$ for $k \in [d]$. Then,*

$$\sum_{i=1}^d \mathbb{E}_q[g_k \cdot (\partial_k \log p_{\boldsymbol{\theta}})(\partial_k \log q)] = - \sum_{k=1}^d \mathbb{E}_q[\partial_k(g_k \partial_k \log p_{\boldsymbol{\theta}})].$$

The proof can be found in [\[Yu et al., 2019\]](#). Using Lemma 1, generalized SM (4) has the tractable expression,

$$\operatorname{FH}_{\mathbf{g}}(q, p_{\boldsymbol{\theta}}) = \sum_{k=1}^d \mathbb{E}_q[g_k \cdot (\partial_k \log p_{\boldsymbol{\theta}})^2] + 2 \sum_{k=1}^d \mathbb{E}_q[\partial_k(g_k \partial_k \log p_{\boldsymbol{\theta}})] + C$$

where C is a constant independent of $\boldsymbol{\theta}$. One can replace the expectation with the empirical mean over X_q to obtain an unbiased estimator of the above objective function. It is straightforward to modify the generalized SM formulation so that it works for doubly truncated distributions. E.g., $g_k(\mathbf{x}) = \min\{x_k - a_k, b_k - x_k\}$ can be used to estimate truncated densities on the product space $\prod_{k=1}^d (a_k, b_k)$.

It is worth pointing out that Lemma 1 is a specification of the divergence theorem such as Green's theorem or Stokes' theorem which usually deals with a bounded V . Recently, [Mardia et al. \[2016\]](#) studied an SM objective based on Stokes' theorem, for estimating densities on a Riemannian manifold.

In this paper, we are interested in estimating a density model defined on a generic, bounded open domain V whose boundary is denoted as ∂V . It is intuitive to think that if we can similarly design a weight function g_k taking 0 at ∂V , an analogue to Lemma 1 would hold, giving a tractable form of the estimator. For example, we can consider a $\operatorname{dist}(\mathbf{x}, \mathbf{z})$, which is a distance function between \mathbf{x} and \mathbf{z} , and let the weight function g_k be

$$g_k = g_0 := \min_{\mathbf{z} \in \partial V} \operatorname{dist}(\mathbf{x}, \mathbf{z}), \quad \forall k \in [d], \mathbf{x} \in \bar{V}. \quad (5)$$

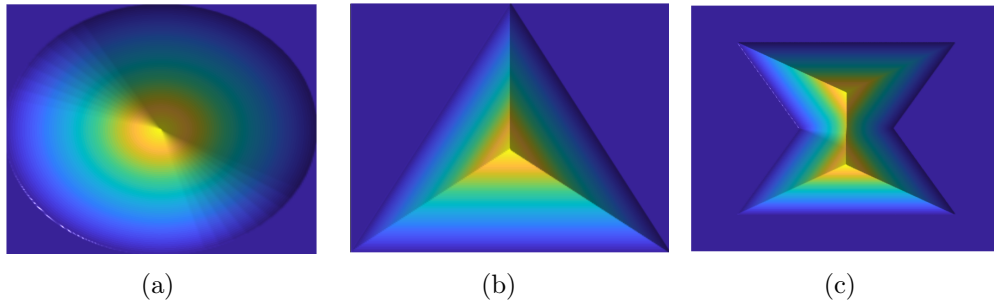


Figure 2: Examples of $g_0(\mathbf{x})$ for (a) a circular boundary (b) a triangular boundary and (c) a polygon boundary. Here $\text{dist}(\cdot, \cdot)$ is the Euclidean distance function.

i.e., the distance from \mathbf{x} to the truncation boundary.

See Figure 2 for examples of g_0 defined on some simple bounded domains V . This weight function is intuitive and can be easily computed for many truncation boundaries (See Section 7 for details).

However, there are still two major concerns: First, it is unclear whether generalized SM using g_0 as the weight function would entail a tractable objective function. Lemma 1 is only derived for the positive orthant and it assumes $g_k(\mathbf{x})$ to be continuous differentiable. However, g_0 is not differentiable everywhere on V . It is also not obvious whether g_0 is differentiable *almost everywhere*¹. Second, the efficacy of g_0 is unclear. The weight function g_k can be an arbitrary function which satisfies the boundary condition (\mathbf{g} taking $\mathbf{0}$ at ∂V). It is not immediately clear why using g_0 as weight function would yield good density estimation performance. In the following sections, we address these two concerns from theoretical and empirical point of views.

We now refer to generalized SM with $g_k = g_0$ as truncated SM, or *TruncSM* for short.

4 Tractable Objective for Truncated Score Matching

First, we study the tractability of the TruncSM objective. The key observation is that g_0 defined on a *Lipschitz domain* is *weakly differentiable*. To show this, let us formally define a Lipschitz domain and the notion of a weakly differentiable function via Sobolev-Hilbert space:

Definition 2 (Lipschitz Domain). *Let V be an open and bounded domain in \mathbb{R}^d . We say V is a **Lipschitz domain** if for any $\mathbf{x} \in \partial V$, there exists an $r > 0$ and a Lipschitz function $f(x_1, \dots, x_{d-1})$ such that $V \cap B(\mathbf{x}, r)$ is expressed by $\{\mathbf{z} \in B(\mathbf{x}, r) \mid z_d > f(z_1, \dots, z_{d-1})\}$ upon a transformation of the coordinate system if necessary. $B(\mathbf{x}, r)$ denotes a d -dimensional ball centered at \mathbf{x} with radius r .*

¹As we will see later, it depends on V .

Intuitively speaking, a Lipschitz domain $V \subset \mathbb{R}^d$ is a bounded open domain whose local boundary is a level set of some Lipschitz function. In engineering applications, most domains are Lipschitz domains. However, it does not include domains with “cracks”.

Definition 3 (Sobolev-Hilbert space). : Let $L^2(V)$ be the L^2 space on $V \subset \mathbb{R}^d$ endowed with the Lebesgue measure. Then, $H^1(V)$ is the Sobolev-Hilbert space defined by

$$H^1(V) = \left\{ f \in L^2(V) \mid \|f\|_{L^2(V)}^2 + \sum_k \|D_k f\|_{L^2(V)}^2 < \infty \right\},$$

where D_k is the weak derivative corresponding to ∂_k and $\|f\|_{L^2(V)} = \sqrt{\int_V |f(\mathbf{x})|^2 d\mathbf{x}}$.

The full definition of the weak derivative and more details about Lipschitz domains and Sobolev-Hilbert spaces can be found in Section 7 of [Atkinson and Han, 2005].

Lemma 2. Suppose V is a Lipschitz domain, then $g_0 \in H^1(V)$.

Proof. First, we show that g_0 is Lipschitz continuous with respect to the metric $\text{dist}(\cdot, \cdot)$.

$$\begin{aligned} \forall \mathbf{x}_a, \mathbf{x}_b \in V, g_0(\mathbf{x}_a) - g_0(\mathbf{x}_b) &= \left(\min_{\mathbf{x}' \in \partial V} \max_{\mathbf{x}'' \in \partial V} \text{dist}(\mathbf{x}_a, \mathbf{x}') - \text{dist}(\mathbf{x}_b, \mathbf{x}'') \right) \\ &\leq \left(\max_{\mathbf{x}'' \in \partial V} \text{dist}(\mathbf{x}_a, \mathbf{x}'') - \text{dist}(\mathbf{x}_b, \mathbf{x}'') \right) \leq \text{dist}(\mathbf{x}_a, \mathbf{x}_b). \end{aligned}$$

The last inequality is due to the triangle inequality. Likewise, $g_0(\mathbf{x}_b) - g_0(\mathbf{x}_a)$ is also bounded above by $\text{dist}(\mathbf{x}_a, \mathbf{x}_b)$. Therefore g_0 is a Lipschitz function with Lipschitz constant 1. Rademacher’s theorem [Evans and Garipey, 1992] asserts that a Lipschitz continuous function is differentiable at every point in a Lipschitz domain outside a set of *measure zero*. Therefore, we can construct

$$D_k g_0(\mathbf{x}) := \begin{cases} \partial_k g_0(\mathbf{x}), & \text{if } g_0 \text{ is differentiable,} \\ \text{arbitrary constant,} & \text{otherwise} \end{cases} \quad (6)$$

We can check that $D_k g_0(\mathbf{x})$ is a valid weak derivative (Definition 7.1.3., [Atkinson and Han, 2005]):

$$\int_V g_0(\mathbf{x}) \partial_k \phi(\mathbf{x}) d\mathbf{x} = - \int_V D_k g_0(\mathbf{x}) \phi(\mathbf{x}) d\mathbf{x},$$

where ϕ is any m -times differentiable function on a compact support in V . The equality holds due to the classic integration by parts formula for continuous differentiable functions. g_0 is only non-differentiable over a zero set, so the arbitrary constant we set in (6) does not affect the outcome of the integration. Since V is a bounded domain and g_0 is 1-Lipschitz, g_0 and $D_k g_0$ are both bounded in terms of the $\|\cdot\|_{L^2(V)}$ norm. Therefore, g_0 is weakly differentiable and in a Sobolev-Hilbert space. \square

Now we would like to prove an analogue of Lemma 1 for all functions in $H^1(V)$. The classic Green's theorem or Stokes' theorem used in Lemma 1 cannot be applied to derive a tractable objective anymore as functions in $H^1(V)$ are *not* differentiable everywhere. However, there exists an extension of Green's theorem of weakly differentiable functions (Proposition 7.6.1 [Atkinson and Han, 2005]).

Theorem 1 (Extended Green's Theorem). *For the Lipschitz domain $V \subset \mathbb{R}^d$, suppose $f_1, f_2 \in H^1(V)$,*

$$\int_V f_1(\mathbf{x}) \partial_k f_2(\mathbf{x}) d\mathbf{x} = \int_{\partial V} f_1(\mathbf{x}) f_2(\mathbf{x}) \nu_k(\mathbf{x}) ds - \int_V f_2(\mathbf{x}) \partial_k f_1(\mathbf{x}) d\mathbf{x}, \quad \forall k \in [d],$$

where (ν_1, \dots, ν_d) is the unit outward normal vector on ∂V and ds is the surface element on ∂V .

Now we use Theorem 1 to derive a tractable form of (4) for weight functions $g_k \in H^1(V)$:

Theorem 2. *Assume $V \subset \mathbb{R}^d$ is a Lipschitz domain. Suppose $q, g_k \partial_k \log p_\theta \in H^1(V)$ and that for any $\mathbf{z} \in \partial V$ it holds that*

$$\lim_{\mathbf{x} \rightarrow \mathbf{z}} q(\mathbf{x}) g_k(\mathbf{x}) \partial_k \log p_\theta(\mathbf{x}) \nu_k(\mathbf{z}) = 0, \forall k \in [d],$$

where $\mathbf{x} \rightarrow \mathbf{z}$ takes any point sequence converging to $\mathbf{z} \in \partial V$ into account. Then, we have

$$\sum_{i=1}^d \mathbb{E}_q [g_i \cdot (\partial_i \log p_\theta) (\partial_i \log q)] = - \sum_{k=1}^d \mathbb{E}_q [\partial_k (g_k \partial_k \log p_\theta)].$$

The proof of the above theorem can be found in Appendix B. Due to Lemma 2, we see that the assumption $g_0 \partial_k \log p_\theta \in H^1(V)$ in Theorem 2 holds as long as $\partial_k \log p_\theta \in H^1(V)$, which is a reasonable assumption for many truncated density models. This indicates that TruncSM indeed has a tractable objective function.

$$\boldsymbol{\theta}_{\text{TSM}} := \underset{\boldsymbol{\theta}}{\operatorname{argmin}} \operatorname{FH}_{g_0}(q, p_\theta),$$

$$\begin{aligned} &= \underset{\boldsymbol{\theta}}{\operatorname{argmin}} \sum_{k=1}^d \mathbb{E}_q [g_0 \cdot (\partial_k \log p_\theta)^2] + 2 \sum_{k=1}^d \mathbb{E}_q [\partial_k (g_0 \partial_k \log p_\theta)] \\ &= \underset{\boldsymbol{\theta}}{\operatorname{argmin}} \sum_{k=1}^d \mathbb{E}_q [g_0 \cdot (\partial_k \log p_\theta)^2] + 2 \sum_{k=1}^d \mathbb{E}_q [g_0 \partial_k^2 \log p_\theta] + 2 \sum_{k=1}^d \mathbb{E}_q [\partial_k g_0 \cdot \partial_k \log p_\theta], \quad (7) \end{aligned}$$

where each expectation can be approximated using samples from the dataset $X_q \sim Q$. Now we turn our focus to the efficacy of TruncSM. In the next section, we show TruncSM is a Minimum Stein Discrepancy Estimator [Barp et al., 2019].

5 Truncated Score Matching as Minimum Stein Discrepancy Estimator

Maximum Stein Discrepancies are a family of discrepancies which measure the differences between two distributions [Chwialkowski et al., 2016, Liu et al., 2016]. For simplicity, we assume that q, ℓ_θ are smooth in this section.

Definition 4. Given an $\mathbf{f} : \mathbb{R}^d \rightarrow \mathbb{R}^d$, a **Stein operator** is defined as

$$T_p \mathbf{f} := \sum_{k=1}^d \{(\partial_k \log p) \cdot f_k + \partial_k f_k\},$$

where $\mathbf{f} = (f_1, \dots, f_d)$, p is a probability density function and $\mathcal{S}_p := \{\mathbf{f} \mid \mathbb{E}_p[T_p \mathbf{f}] = 0\}$ is called a **Stein class** of p . The Maximum Stein Discrepancy between two densities q and p [Chwialkowski et al., 2016, Liu et al., 2016] is defined as $\max_{\mathbf{f} \in \mathcal{S}_p} \mathbb{E}_q [T_p \mathbf{f}]$.

By constructing different Stein classes \mathcal{S}_p , we obtain different Maximum Stein Discrepancies.

Since our task is estimating a parametric density model p_θ , we can consider a density estimator that minimizes this discrepancy, i.e., $\underset{\theta}{\operatorname{argmin}} \max_{\mathbf{f} \in \mathcal{S}_{p_\theta}} \mathbb{E}_q [T_{p_\theta} \mathbf{f}]$, and this estimator has been shown to be effective, robust, and closely related to SM and is called Minimum Stein Discrepancy Estimator [Barp et al., 2019].

When using the above estimator, the key issue is constructing a Stein class \mathcal{S}_{p_θ} which is expressive enough to capture subtle differences between q and p_θ . In the following theorem, we construct a Stein class with \mathbf{f} that are the product of a smooth function and a Lipschitz function. We show the Maximum Stein Discrepancy using this specific Stein class becomes FH divergence weighted by g_0 .

First we introduce a Lemma whose proof can be found in Appendix C.1.

Lemma 3. Let $\operatorname{Lip}_0^L(V)$ be the set of all functions $f : \bar{V} \rightarrow \mathbb{R}$

- that are L -Lipschitz continuous with respect to $\operatorname{dist}(\cdot, \cdot)$
- satisfies the property that $f(\mathbf{x}) = 0, \forall \mathbf{x} \in \partial V$

then $\max_{g_k \in \operatorname{Lip}_0^L, \forall k \in [d]} \operatorname{FH}_g(q, p_\theta) = L \cdot \operatorname{FH}_{g_0}(q, p_\theta)$.

Theorem 3. Let \mathcal{F} be a function class such that $\forall \mathbf{f} \in \mathcal{F}, \mathbf{f} = \mathbf{h} \circ \mathbf{g}^{1/2}$ and $\mathbb{E}_q \|\mathbf{h}(\mathbf{x})\|^2 \leq 1$, where $\mathbf{h} : \bar{V} \rightarrow \mathbb{R}^d$ is a smooth function and $\forall k, g_k \in \operatorname{Lip}_0^L(V)$ then

- \mathcal{F} is a Stein class of a smooth density q defined on V .
- If $\partial_k \ell_\theta$ is smooth with respect to θ for all k , we have $\max_{\mathbf{f} \in \mathcal{F}} \mathbb{E}_q [T_{p_\theta} \mathbf{f}] = \sqrt{L \cdot \operatorname{FH}_{g_0}(q, p_\theta)}$.

The proof can be found in Appendix C.2 and it is partly based on the proof Theorem 2 in Barp et al. [2019]. Theorem 3 shows that the TruncSM objective is a Maximum Stein Discrepancy thus θ_{TSM} is a Minimum Stein Discrepancy Estimator.

Similarly, we can show how a ‘‘capped’’ g_0 arises by choosing a slightly different family for g_k in Theorem 3. We find this capped weight function can be also effective in many tasks (see Section 6.3 and 8.2).

Corollary 1. *Let us define $\overline{\text{Lip}}_0^L(V) := \{f \in \text{Lip}_0^L(V) | f(\mathbf{x}) \leq 1\}$, and let g_k in Theorem 3 be $g_k \in \overline{\text{Lip}}_0^L(V)$, then*

$$\max_{\mathbf{f} \in \mathcal{F}} \mathbb{E}_q [T_{p\theta} \mathbf{f}] = \sqrt{\text{FH}_{\bar{g}_L}(q, p\theta)},$$

where $\bar{g}_L = \min(1, L \cdot g_0)$.

The proof can be found in Appendix C.3.

Yu et al. [2019] proposed to use a weight function $g_k = \min(1, x_k), k = 1, \dots, d$ for estimating density functions defined on the positive orthant. This weight function is the special case of \bar{g}_L when V is the entire positive orthant. We refer to \bar{g}_L as a ‘‘capped weight function’’. The capped weight function is discussed in the recent paper by Yu et al. [2020] in the context of generalized SM for the unbounded V .

In the following sections, we investigate the efficacy of TruncSM through theoretical analysis and empirical experiments.

6 Finite Sample Statistical Guarantee of Generalized Score Matching

Now, we study the finite sample statistical guarantee of generalized SM. Using this guarantee, we can see the advantage of using TruncSM in truncated density estimation. There have been studies on the *asymptotic accuracy* of generalized SM in, for example, [Yu et al., 2019] and [Barp et al., 2019]. However, it is hard to study the impact of weight functions from the asymptotic variance due to its complicated expression.

We first establish an estimation error bound for generalized SM using a generic weight function \mathbf{g} . For the convenience of discussion in this section, let us rewrite the generalized SM objective function as

$$M(\theta) = \mathbb{E}_q[m_\theta(\mathbf{x})], \text{ where } m_\theta(\mathbf{x}) := \sum_{k=1}^d \left\{ \underbrace{[(\partial_k \ell_\theta)^2 + 2\partial_k^2 \ell_\theta]}_{=: A_k(\mathbf{x}; \theta)} g_k + \underbrace{2\partial_k \ell_\theta}_{=: B_k(\mathbf{x}; \theta)} \partial_k g_k \right\}, \quad (8)$$

where we abbreviated $\log p_\theta$ as ℓ_θ . It holds that $\text{FH}_{\mathbf{g}}(q, p\theta) = M(\theta) + C$ in which C is independent of θ . Given finite samples $X_q \sim Q$, $M(\theta)$ is approximated by the empirical

mean:

$$\hat{M}(\boldsymbol{\theta}) = \frac{1}{n} \sum_{i=1}^n m_{\boldsymbol{\theta}}(\mathbf{x}_i).$$

Then $\hat{\boldsymbol{\theta}}$, the minimizer of $\hat{M}(\boldsymbol{\theta})$ s.t. $\boldsymbol{\theta} \in \Theta \subset \mathbb{R}^r$ is an M-estimator [van der Vaart, 2000] with the estimation function $m_{\boldsymbol{\theta}}(\mathbf{x})$.

6.1 Non-Asymptotic Error Bound

We first establish the non-asymptotic error bound of the generalized SM procedure (8). Let $\boldsymbol{\theta}^* \in \Theta$ be the minimizer of $M(\boldsymbol{\theta})$ over Θ . We assume that the optimal parameter $\boldsymbol{\theta}^*$ is well-separated from other neighbouring parameters in terms of the population objective values:

Assumption 1. Assume that there exists $\alpha > 1$ such that

$$\inf_{\boldsymbol{\theta}: \|\boldsymbol{\theta} - \boldsymbol{\theta}^*\| \geq \delta} M(\boldsymbol{\theta}) - M(\boldsymbol{\theta}^*) \geq C_{\mathbf{g}} \delta^\alpha \quad (9)$$

holds for any small $\delta > 0$. Here, $C_{\mathbf{g}}$ is a positive constant that may depend on the weight function \mathbf{g} such that $C_{a\mathbf{g}} = aC_{\mathbf{g}}$ for any positive constant a .

When $M(\boldsymbol{\theta})$ is twice differentiable with respect to $\boldsymbol{\theta}$ and the Hessian matrix of $M(\boldsymbol{\theta})$ is non-degenerate for all $\boldsymbol{\theta} \in \Theta$, $\alpha = 2$ holds in (9).

Assumption 2. The sequence $\hat{\boldsymbol{\theta}}$ converges to $\boldsymbol{\theta}^*$ in probability.

The consistency of M -estimator has been well-studied in the statistical literature, thus we do not discuss in detail. Here we are only interested in the rate that governs the convergence of $\hat{\boldsymbol{\theta}}$ and its implication on choosing g_k . A set of sufficient conditions for proving the consistency of $\hat{\boldsymbol{\theta}}$ is discussed in Theorem 5.7 of van der Vaart [2000].

We also make continuity assumptions on $m_{\boldsymbol{\theta}}(\mathbf{x})$. This is needed to ensure the upper-boundedness of the covering number when proving the convergence rate.

Assumption 3. For the function A_k and B_k in $m_{\boldsymbol{\theta}}(\mathbf{x})$, there exists $\dot{A}_k, \dot{B}_k, \forall k$ such that

$$\begin{aligned} |A_k(\mathbf{x}, \boldsymbol{\theta}_1) - A_k(\mathbf{x}, \boldsymbol{\theta}_2)| &\leq \dot{A}_k(\mathbf{x}) \|\boldsymbol{\theta}_1 - \boldsymbol{\theta}_2\|, \\ |B_k(\mathbf{x}, \boldsymbol{\theta}_1) - B_k(\mathbf{x}, \boldsymbol{\theta}_2)| &\leq \dot{B}_k(\mathbf{x}) \|\boldsymbol{\theta}_1 - \boldsymbol{\theta}_2\|. \end{aligned} \quad (10)$$

If $A_k(\mathbf{x}, \boldsymbol{\theta})$ is differentiable with respect to $\boldsymbol{\theta}$ for all k , due to Taylor expansion and Schwarz inequality, we see $A_k(\mathbf{x}, \boldsymbol{\theta}_1) - A_k(\mathbf{x}, \boldsymbol{\theta}_2) \leq \sup_{\boldsymbol{\theta} \in \Theta} \|\nabla_{\boldsymbol{\theta}} A_k(\mathbf{x}, \boldsymbol{\theta})\| \cdot \|\boldsymbol{\theta}_1 - \boldsymbol{\theta}_2\|$. Applying the same argument to $B_k(\mathbf{x}, \boldsymbol{\theta})$, we can see that both $\dot{A}_k := \sup_{\boldsymbol{\theta} \in \Theta} \|\nabla_{\boldsymbol{\theta}} A_k(\mathbf{x}, \boldsymbol{\theta})\|_2$ and $\dot{B}_k := \sup_{\boldsymbol{\theta} \in \Theta} \|\nabla_{\boldsymbol{\theta}} B_k(\mathbf{x}, \boldsymbol{\theta})\|_2$ would satisfy Assumption 3.

Let us define a function $\Gamma(\mathbf{g}; A, B)$ using \dot{A}_k and \dot{B}_k :

$$\Gamma(\mathbf{g}; A, B) := \sum_{k=1}^d \left\{ (\mathbb{E}_q[\dot{A}_k^4] \mathbb{E}_q[g_k^4])^{1/4} + (\mathbb{E}_q[\dot{B}_k^4] \mathbb{E}_q[(\partial_k g_k)^4])^{1/4} \right\}, \quad (11)$$

then we have the following non-asymptotic estimation error bound of generalized SM:

Theorem 4. *Suppose that Assumptions 1, 3, and 2 hold and that $g_k, \partial_k g_k, \dot{A}$ and \dot{B} have the fourth order moment under the population distribution q . Then for $\varepsilon > 2^{\alpha-1}/\sqrt{r}$ we have*

$$P\left(\|\hat{\boldsymbol{\theta}} - \boldsymbol{\theta}^*\| \geq \left(\varepsilon\sqrt{\frac{r}{n}}\right)^{1/(\alpha-1)}\right) \leq \frac{CK_\alpha}{\varepsilon} \cdot \frac{\Gamma(\mathbf{g}; A, B)}{C_{\mathbf{g}}}, \quad (12)$$

where C is a universal constant and $K_\alpha = \frac{2^{2\alpha}}{2^{\alpha-1}-1}$.

The proof can be found in Appendix D.1. In the proof, we use the convergence analysis of the M-estimator according to Section 5.8 in [van der Vaart, 2000]. If $\alpha = 2$, the estimation error $\|\hat{\boldsymbol{\theta}} - \boldsymbol{\theta}^*\|$ is of the order $\sqrt{\frac{r}{n}}$, which is typical in parametric statistical inference.

Our upperbound on the RHS of (12) does not change if g_k is enlarged L times: enlarging g_k L times will enlarge both $\Gamma(\mathbf{g}; A, B)$ and $C_{\mathbf{g}}$ by L times.

Most importantly, Theorem 4 shows how the choice of weight \mathbf{g} affects the convergence from $\hat{\boldsymbol{\theta}}$ to $\boldsymbol{\theta}^*$. The only term involves \mathbf{g} on the RHS of (12) is $\frac{\Gamma(\mathbf{g}; A, B)}{C_{\mathbf{g}}}$. Naturally, we would like to choose a \mathbf{g} such that $\frac{\Gamma_{\mathbf{g}}}{C_{\mathbf{g}}}$ is minimized². Some details will be discussed in Section 6.2 and Appendix E.

Note that the optimal parameter $\boldsymbol{\theta}^*$ depends on weight function \mathbf{g} , thus it does not make sense to analyze the convergence rate while $\boldsymbol{\theta}^*$ keeps changing. In the following section, we assume there exists a unique $\boldsymbol{\theta}^*$ such that $p_{\boldsymbol{\theta}^*} = q$ and $\text{FH}_{\mathbf{g}}(q, \boldsymbol{\theta}^*) \equiv 0$ for all \mathbf{g} , i.e., the model is correctly specified by a unique parameter $\boldsymbol{\theta}^*$.

6.2 Choice of Weight Function

We cannot minimize $\frac{\Gamma_{\mathbf{g}}}{C_{\mathbf{g}}}$ with respect to \mathbf{g} analytically, as we do not know $q(\mathbf{x})$ and the closed form expressions of \dot{A}_k or \dot{B}_k . Numerical minimization of $\frac{\Gamma_{\mathbf{g}}}{C_{\mathbf{g}}}$ can also be cumbersome. Instead, we present a lightweight selection procedure, which eventually gives rise to the weight function g_0 used by TruncSM.

Suppose we would like to control $\frac{\Gamma_{\mathbf{g}}}{C_{\mathbf{g}}}$ with respect to $\mathbf{g} \in \mathcal{G}$ and there exists a constant $\Gamma_{\mathcal{G}} \geq \sup_{\mathbf{g} \in \mathcal{G}} \Gamma_{\mathbf{g}}$. We obtain an upperbound $\frac{\Gamma_{\mathcal{G}}}{C_{\mathbf{g}}} \geq \frac{\Gamma_{\mathbf{g}}}{C_{\mathbf{g}}}$. The choice of \mathcal{G} is important as $\Gamma_{\mathcal{G}}$ may not exist or be very large for some \mathcal{G} . However (11) suggests, as long as $|\partial_k g_k|$ and $|g_k|$ are upperbounded and \dot{A}_k and \dot{B}_k are well behaved, $\Gamma_{\mathcal{G}}$ should exist. Let us consider

$$\mathcal{G} := \{\mathbf{g} \in \mathbb{R}^d | g_k \in \text{Lip}_0^1(V), \forall k \in [d]\}.$$

We can see $\forall \mathbf{g} \in \mathcal{G}, |\partial_k g_k| \leq 1$ due to the property of Lipschitz function and $|g_k|$ is bounded as it is defined over a bounded domain. Note we have used Lipschitz functions to construct a Stein class in Section 5, here Lipschitz functions emerge from a different context: Upperbounding the estimation error.

After fixing \mathcal{G} , we seek to maximize the denominator $C_{\mathbf{g}}$ by choosing an appropriate $\mathbf{g} \in \mathcal{G}$. Let us introduce the following proposition:

²For simplicity, let us shorten $\Gamma(\mathbf{g}; A, B)$ as $\Gamma_{\mathbf{g}}$ from now on.

Proposition 1. *Given the \mathcal{G} defined above, suppose $q = p_{\theta^*}$, then*

$$\inf_{\theta: \|\theta - \theta^*\| \geq \delta} M_{g_0}(\theta) - M_{g_0}(\theta^*) \geq \sup_{\mathbf{g} \in \mathcal{G}} \inf_{\theta: \|\theta - \theta^*\| \geq \delta} M_{\mathbf{g}}(\theta) - M_{\mathbf{g}}(\theta^*),$$

where $M_{\mathbf{g}}(\theta)$ is $M(\theta)$ using \mathbf{g} as weight function.

Proof.

$$\begin{aligned} & \inf_{\theta: \|\theta - \theta^*\| \geq \delta} M_{g_0}(\theta) - M_{g_0}(\theta^*) \\ &= \inf_{\theta: \|\theta - \theta^*\| \geq \delta} \text{FH}_{g_0}(\theta) - \text{FH}_{g_0}(\theta^*) \\ &= \inf_{\theta: \|\theta - \theta^*\| \geq \delta} \sup_{\mathbf{g} \in \mathcal{G}} \text{FH}_{\mathbf{g}}(\theta) - \text{FH}_{\mathbf{g}}(\theta^*) \\ &= \inf_{\theta: \|\theta - \theta^*\| \geq \delta} \sup_{\mathbf{g} \in \mathcal{G}} M_{\mathbf{g}}(\theta) - M_{\mathbf{g}}(\theta^*) \geq \sup_{\mathbf{g} \in \mathcal{G}} \inf_{\theta: \|\theta - \theta^*\| \geq \delta} M_{\mathbf{g}}(\theta) - M_{\mathbf{g}}(\theta^*). \end{aligned}$$

The second equality is due to Lemma 3 and by assumption $\text{FH}_{\mathbf{g}}(\theta^*) \equiv 0, \forall \mathbf{g}$. The inequality is due to max-min inequality. \square

Proposition 1 shows, when using $\mathbf{g}_0 := (g_0, \dots, g_0)$ as the weight function, Assumption 1 should hold for a constant $C_{g_0} = \sup_{\mathbf{g} \in \mathcal{G}} C_{\mathbf{g}}$. Since \mathbf{g}_0 is in \mathcal{G} (Lemma 2), we can see \mathbf{g}_0 maximizes $C_{\mathbf{g}}$ for all $\mathbf{g} \in \mathcal{G}$. As $\Gamma_{\mathcal{G}}$ does not depend on any individual \mathbf{g} , this means \mathbf{g}_0 minimizes the upper bound $\frac{\Gamma_{\mathcal{G}}}{C_{\mathbf{g}}}$.

Note that we can reach a similar conclusion by replacing \mathcal{G} to $\bar{\mathcal{G}} := \{\mathbf{g} \in \mathbb{R}^d | g_k \in \overline{\text{Lip}}_0^1(V), \forall k \in [d]\}$ and the minimizer of $\frac{\Gamma_{\bar{\mathcal{G}}}}{C_{\mathbf{g}}}$ would change from g_0 to the capped distance \bar{g}_L .

Here we do *not* claim that g_0 or \bar{g}_L is *the best* weight function for estimating truncated densities using generalized SM. (9) and (11) suggest that there should be other data-driven choices of \mathbf{g} that yield better error bounds. However, g_0 should be an adequate choice judging from our estimation error upper bound. Finding a tractable data-driven \mathbf{g} that minimizes the estimation error bound is an interesting future work.

6.3 Case Study: Truncated Density in a Unit Ball

In this section, we study a case where q has a parametric form and V is a unit ball. Although this is a very specific setting, we can see how the relationship between q , V and different choices of \mathbf{g} would influence the error bound. In what follows, we consider the capped weight function $\bar{g}_L(\mathbf{x}) = \min\{Lg_0(\mathbf{x}), 1\}$ which has been introduced in Corollary 1. g_0 is defined using the euclidean distance.

Let us define $p_{\text{dist}}(z)$ as the probability density of $Z = g_0(X)$ for $X \sim q$. For simplicity, we assume that there exist positive constants b and b' such that $bz^\beta \leq p_{\text{dist}}(z) \leq b'z^\beta$ holds for $0 < z \leq c$, where c and β are constants. Note that β should be greater than -1 since the integral of $p_{\text{dist}}(z)$ on the interval $(0, c)$ should be bounded.

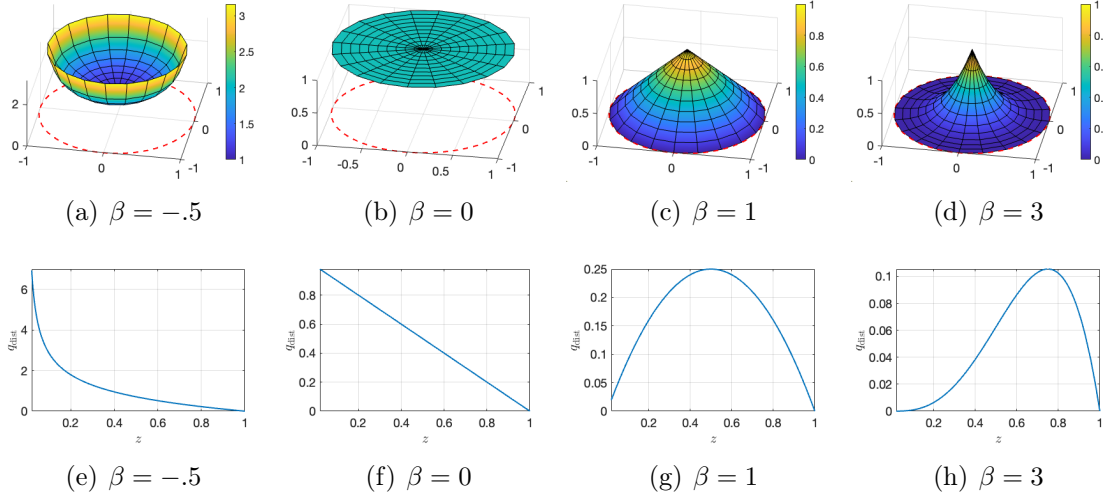


Figure 3: Top row: unnormalized q_β , where ∂V in Example 1 is illustrated using a red dashed line. Bottom row: unnormalized $p_{\text{dist}}(z; \beta)$ in Example 1.

Example 1. Let V be the unit open ℓ^2 ball in \mathbb{R}^d , i.e., $V = \{\mathbf{x} \in V \mid \|\mathbf{x}\| < 1\}$. We consider the distribution $q_\beta(\mathbf{x}) \propto (1 - \|\mathbf{x}\|)^\beta$ on V , where $\beta > -1$. Then, we have $p_{\text{dist}}(z) \propto (1 - z)^{d-1} z^\beta$, $0 < z \leq 1$. For a small z , we have $bz^\beta \leq p_{\text{dist}}(z) \leq b'z^\beta$.

See Figure 3 for illustrations of unnormalized q_β and $p_{\text{dist}}(z; \beta)$. It can be seen that:

- If $q(\mathbf{x})$ converges to a positive constant as $\mathbf{x} \rightarrow \partial V$, $\beta = 0$.
- If $q(\mathbf{x})$ tends to zero, as $\mathbf{x} \rightarrow \partial V$, $\beta > 0$.
- If $q(\mathbf{x})$ tends to infinity, as $\mathbf{x} \rightarrow \partial V$, $\beta < 0$.

For $\beta > -1$ and $L \geq \max\{1, 1/c\}$, where c is independent of L , we have the bounds for $\frac{\Gamma_{\bar{g}_L}}{C_{\bar{g}_L}}$:

$$C_A \left(1 - \frac{C_{b',\beta}}{L^{\beta+1}}\right)^{1/4} + C_B c_0 L^{(1-\beta)/2} \leq \frac{\Gamma_{\bar{g}_L}}{C_{\bar{g}_L}} \leq C_A \left(1 - \frac{c_{b,\beta}}{L^{\beta+1}}\right)^{1/4} + C_B c_1 L^{(3-\beta)/4}, \quad (13)$$

where $c_0, c_1, c_{b,\beta}, C_{b',\beta}, C_A, C_B$ are positive constants independent of L . The first term of the lower and upper bounds is positive for $L \geq 1$. The detailed derivation of this bound is found in Appendix F. Although we assume that p_{dist} takes a specific form in this example, the derivation mostly concerns the behavior of $p_{\text{dist}}(z)$, $z < c$. Thus a slight modification of (13) should cover a different pair of p_{dist} and q_β that has the same behavior near the boundary.

First, let us consider the condition $\beta > 3$ in which case $q(\mathbf{x})$ rapidly goes to zero as \mathbf{x} converges to a point on the boundary of V . The upper and lower bounds in (13) converge to C_A as L tends to infinity, meaning that a large L does guarantee a reasonable accuracy. When $\beta > 3$, $q(\mathbf{x})$ is almost zero around the boundary (see Figure 3), so the truncation

should not play a big role in density estimation. By setting L to a large value, TruncSM with \bar{g}_L is essentially the classic SM which is well-suited for non-truncated density estimation.

On the other hand, when q_β goes to zero slowly ($0 < \beta \leq 1$) or converges to a constant at the boundary ($\beta \leq 0$), a larger L leads to a larger lower bound, which is undesirable. In particular, when $\beta < 0$, increasing L will increase both upper and lowerbound rapidly. This implies a smaller L would yield a better performance when β is small.

Our analysis can also be visually validated via Figure 3: When β is large, p_{dist} is low around the boundary, thus a steep g_0 (i.e., large L) near the boundary would not blow up $\Gamma_{\mathbf{g}}$ (which depends on $E_q[(\partial_k g_k)^4] \leq L^4$). However, as we reduce β , p_{dist} takes higher values near the boundary. A steep \bar{g}_L near the boundary would lead to a large $\Gamma_{\mathbf{g}}$, hence a larger estimation error.

For the truncated distribution on the bounded domain such as the truncated Gaussian (or Gaussian mixture) model, the probability density $p_{\text{dist}}(z)$ is greater than a positive constant near the boundary. The above analysis shows that the capped distance function efficiently works for such truncated probability models.

7 Computation of g_0

Comparing to other choices of weight functions, g_0 (and \bar{g}_L) have an important advantage: the computation of g_0 and its gradient can be efficiently carried out for properly defined V .

For example, if V and ∂V are expressed by $V = \{\mathbf{x} \in \mathbb{R}^d | u(\mathbf{x}) < 0\}$ and $\partial V = \{\mathbf{x} \in \mathbb{R}^d | u(\mathbf{x}) = 0\}$ using a function $u : V \rightarrow \mathbb{R}$, evaluating $g_0(\mathbf{x})$ can be turned into an optimization problem: $g_0(\mathbf{x}) = \min_{\mathbf{z}} \{\text{dist}(\mathbf{x}, \mathbf{z}) | u(\mathbf{z}) = 0\}$. In addition, if Euclidean distance is considered, the gradient of $g_0(\mathbf{x})$ is simply given by $\nabla_{\mathbf{x}} g_0(\mathbf{x}) = (\mathbf{x} - \tilde{\mathbf{x}}) / \|\mathbf{x} - \tilde{\mathbf{x}}\|$, where $\tilde{\mathbf{x}}$ is the minimizer of $\min_{\mathbf{z} \in \partial V} \|\mathbf{x} - \mathbf{z}\|$.

We only need to evaluate g_0 and $\partial_k g_0$ *exactly once* for all $\mathbf{x} \in X_q$ *before* estimating $\hat{\boldsymbol{\theta}}$, since g_0 is model agnostic. This can be advantageous when $\bar{p}_{\boldsymbol{\theta}}$ is a sophisticated model and the optimization for $\boldsymbol{\theta}$ is time-consuming. In contrast, if one uses Monte Carlo methods (e.g. Kannan et al. [1997]) to approximate the normalizing constant $Z_V(\boldsymbol{\theta})$ in MLE, they are required to update the estimate of $Z_V(\boldsymbol{\theta})$ throughout the entire optimization procedure. Approximating $Z_V(\boldsymbol{\theta})$ using Markov Chain Monte Carlo (MCMC) can also get less efficient both in terms of statistical accuracy and computation as dimensionality increases. Moreover, some algorithms designed for multivariate Gaussian densities, such as the ones proposed by Daskalakis et al. [2018, 2019], do not require exhaustive sampling. However, they need to evaluate a membership oracle (if $\mathbf{x} \in V$ or not) many times over the course of the optimization. In a high dimensional space, the evaluation of the membership function can be complicated if not as complicated as calculating g_0 .

In what follows, we show efficient analytical methods for computing the distance function defined over *unit ball*, *unit cube*, *convex polytopes* and *polygons*.

- For the Unit Ball, $V = \{\mathbf{x} \in \mathbb{R}^d | \|\mathbf{x}\| < 1\}$, the distance function and its gradient:

$$g_0(\mathbf{x}) = 1 - \|\mathbf{x}\|, \nabla_{\mathbf{x}} g_0(\mathbf{x}) = \frac{-\mathbf{x}}{\|\mathbf{x}\|}.$$

- For the Unit Cube, $V = \{\mathbf{x} \in \mathbb{R}^d \mid \|\mathbf{x}\|_\infty < 1\}$, the distance function and its gradient:

$$g_0(\mathbf{x}) = 1 - \|\mathbf{x}\|_\infty, \quad \nabla_{\mathbf{x}} g_0(\mathbf{x}) = -\mathbf{e}_k, \quad k = \operatorname{argmax}_j |x_j|.$$

- For the Convex Polytope $V = \{\mathbf{x} \in \mathbb{R}^d \mid \langle \mathbf{a}_t, \mathbf{x} \rangle + b_t < 0, t = 1, \dots, T\}$, the distance function is given by

$$g_0(\mathbf{x}) = \min_{\mathbf{z}} \{\|\mathbf{x} - \mathbf{z}\| \mid \max_{t \in [T]} \{\langle \mathbf{a}_t, \mathbf{z} \rangle + b_t\} = 0\} = \min_{t \in [T]} \frac{|\langle \mathbf{a}_t, \mathbf{x} \rangle + b_t|}{\|\mathbf{a}_t\|} \quad (14)$$

for $\mathbf{x} \in V$. The envelope theorem [Milgrom and Segal, 2002] yields $\nabla_{\mathbf{x}} g_0(\mathbf{x}) = -\mathbf{a}_{t^*} / \|\mathbf{a}_{t^*}\|$, where $t^* \in [T]$ is the minimizer of (14). Bric [1997] studied another representation of the minimum distance problem for the convex polyhedral using the extreme points. Note that if V is not a convex set, (14) cannot be used.

- For the Convex Polytope $V = \{\mathbf{x} \in \mathbb{R}^d \mid \langle \mathbf{a}_t, \mathbf{x} \rangle + b_t < 0, t = 1, \dots, T\}$, let us compute the ℓ^1 -based distance function $g_0(\mathbf{x}) = \min_{\mathbf{z} \in \partial V} \|\mathbf{x} - \mathbf{z}\|_1$ for $\mathbf{x} \in V$. It holds that $g_0(\mathbf{x}) = \max\{\alpha \mid \mathbf{x} + \alpha \mathbf{e}_i \in V, \forall i\}$ since V is convex. The condition $\mathbf{x} + \alpha \mathbf{e}_i \in V, \forall i$ is expressed by $\alpha \langle \mathbf{a}_t, \mathbf{e}_i \rangle \leq -\langle \mathbf{a}_t, \mathbf{x} \rangle - b_t$ for all t and i . Hence, we have

$$g_0(\mathbf{x}) = \min_{i, t \text{ s.t. } \langle \mathbf{a}_t, \mathbf{e}_i \rangle \neq 0} \left| \frac{\langle \mathbf{a}_t, \mathbf{x} \rangle + b_t}{\langle \mathbf{a}_t, \mathbf{e}_i \rangle} \right| = \min_{t \in [T]} \frac{|\langle \mathbf{a}_t, \mathbf{x} \rangle + b_t|}{\|\mathbf{a}_t\|_\infty}. \quad (15)$$

The envelope theorem [Milgrom and Segal, 2002] yields $\nabla_{\mathbf{x}} g_0(\mathbf{x}) = -\mathbf{a}_{t^*} / \|\mathbf{a}_{t^*}\|_\infty$ for $\mathbf{x} \in V$, where $t^* \in [T]$ is the minimizer of the last minimization in (15).

- For the Polygon V in \mathbb{R}^2 surrounded by the points $\mathbf{p}_1, \mathbf{p}_2, \dots, \mathbf{p}_T \in \mathbb{R}^2$, the boundary is given by $\partial V = \cup_{t=1}^T \{\alpha \mathbf{p}_t + (1 - \alpha) \mathbf{p}_{t+1} \mid \alpha \in [0, 1]\}$, where $\mathbf{p}_{T+1} = \mathbf{p}_1$. Hence we have

$$g_0(\mathbf{x}) = \min_{t \in [T]} \min_{\alpha: 0 \leq \alpha \leq 1} \|\mathbf{x} - \alpha \mathbf{p}_t - (1 - \alpha) \mathbf{p}_{t+1}\|.$$

The minimizer of the inner optimization is $\alpha_t = \min\{1, \max\{0, \frac{\langle \mathbf{p}_t - \mathbf{p}_{t+1}, \mathbf{x} - \mathbf{p}_{t+1} \rangle}{\|\mathbf{p}_t - \mathbf{p}_{t+1}\|^2}\}\}$. Hence, we obtain $g_0(\mathbf{x}) = \min_{t \in [T]} \|\mathbf{x} - \alpha_t \mathbf{p}_t - (1 - \alpha_t) \mathbf{p}_{t+1}\|$, and $\nabla_{\mathbf{x}} g_0(\mathbf{x}) = \mathbf{n} / \|\mathbf{n}\|$, where $\mathbf{n} = \mathbf{x} - \alpha_{t^*} \mathbf{p}_{t^*} - (1 - \alpha_{t^*}) \mathbf{p}_{t^*+1}$ and where $t^* \in [T]$ the minimizer of $g_0(\mathbf{x})$.

In these cases, the computation of g_0 can be done in polynomial time with respect to d (if T in convex polytope is a polynomial function of d).

8 Numerical and Real-world Data Analysis

To demonstrate the efficacy of TruncSM empirically, we conduct a wide range of experiments. In this section, we use the Euclidean metric for g_0 and \bar{g}_L . The code/datasets to reproduce our experiments are available at <https://github.com/anewgithubname/Truncated-Score-Matching>.

8.1 Illustrative Example and Computation Time

In the first experiment, we show an illustrative example comparing TruncSM, classic MLE and the Rejection Sampling MLE (RJ-MLE), as well as their computational times. Samples are generated from a Gaussian mixture on \mathbb{R}^2 , with centers at

$$\boldsymbol{\mu}_1 = [2, 2], \quad \boldsymbol{\mu}_2 = [-2, 2], \quad \boldsymbol{\mu}_3 = [-2, -2], \quad \boldsymbol{\mu}_4 = [2, -2].$$

The pre-truncated dataset can be seen in Figure 4(a) as black dots. To create a truncated dataset, we limit our observation window to be a green polygon region in the middle, thus only samples inside the green polygon (blue points) can be observed. The task is to find all four centers of the mixture model using *only blue points*. We generate 10000 samples and only 1417 within the truncation boundary can be used for parameter estimation. Our unnormalized density model is a Gaussian mixture model with four components (parametrized by $\boldsymbol{\theta}_1, \dots, \boldsymbol{\theta}_4$) and the unit variance-covariance matrix: $\bar{p}_{\boldsymbol{\theta}_1, \dots, \boldsymbol{\theta}_4}(\mathbf{x}) = \sum_{i=1}^4 \mathcal{N}_{\mathbf{x}}(\boldsymbol{\theta}_i, \mathbf{I})$.

As the boundary ∂V of the non-convex domain V in \mathbb{R}^2 consists of line segments, the analytical algorithm in Section 7 is available to compute g_0 and $\nabla_{\mathbf{x}}g_0$ efficiently. We compare with RJ-MLE which uses rejection sampling to approximate the normalizing constant $Z_V(\boldsymbol{\theta}) := \int_V \bar{p}_{\boldsymbol{\theta}_1, \dots, \boldsymbol{\theta}_4}(\mathbf{x})d\mathbf{x}$. In this experiment, 500000 particles are used to approximate $Z_V(\boldsymbol{\theta})$ and they are drawn from a bivariate uniform distribution with density $\mathcal{U}_{x_1}(-2, 2) \cdot \mathcal{U}_{x_2}(-2, 2)$. The estimated mixture component centers are plotted as green crosses (RJ-MLE) and red dots (TruncSM) in Figure 4(a). It can be seen that both methods give estimates close to the true mixture centers. However, the computation time for TruncSM and RJ-MLE are 0.35 seconds and 3.35 seconds respectively³.

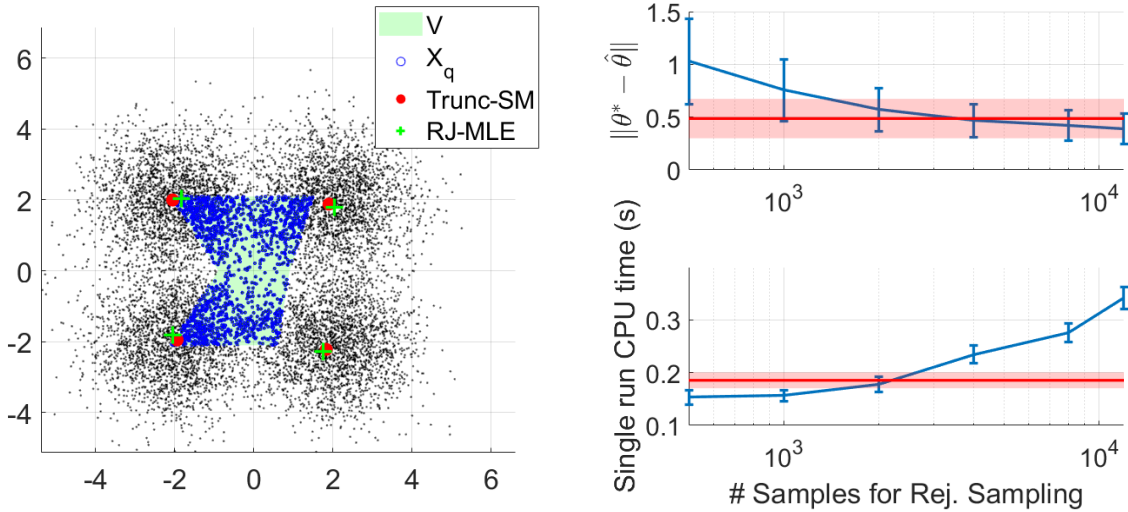
It is worth noting that our particle distribution is carefully chosen so that it tightly covers the truncation domain. It ensures the best rejection sampling performance: Over-coverage would increase the computational cost and insufficient coverage would lower the approximation accuracy of $Z_V(\boldsymbol{\theta})$. While in lower dimensional space, the visualization helps, in a higher dimensional space, it is unclear how to come up with a good rejection sampling distribution.

To further investigate the computation time between TruncSM and RJ-MLE, we study the estimation accuracy and computation time against the number of particles used for rejection sampling by RJ-MLE. We optimize both objective functions using MATLAB's `fminunc` function with default settings. From Figure 4(b), we can see that when using a large number of particles to approximate $Z_V(\boldsymbol{\theta})$, RJ-MLE can indeed achieve a slightly better performance than TruncSM. However, such a slight improvement of estimation accuracy comes with a significant penalty in computation cost even with an optimal choice of the particle distribution.

8.2 Capped Weight Function

Now we investigate the performance of a capped weight function: $\bar{g}_L := \min(1, L \cdot g_0(\mathbf{x}))$. It can be seen that when L is small, \bar{g}_L will never be capped, thus it is equivalent to g_0 after

³For TruncSM, we include the calculation time for g_0 and $\partial_k g_k$. Same below.



(a) Estimation of truncated Gaussian mixture centers (b) Computational cost and estimation accuracy comparison for TruncSM and RJ-MLE

Figure 4: Gaussian mixture centers truncated by a polygon

multiplying a constant, which does not affect the estimator. In this experiment, two different truncation domains are used: a single rectangle and two disjoint rectangles. 1600 samples are drawn from a normal distribution $\mathcal{N}([1, 1], \mathbf{I})$. We monitor the performance of TruncSM using \bar{g}_L as the weight function as V grows in size. We measure the growth of V using a scaling factor b (see Appendix H on how polygons are re-scaled).

Figure 5 shows that as the area of V grows, $\bar{g}_L(\mathbf{x})$ becomes capped for more and more samples in our dataset. This is expected as the boundary stretches, fewer and fewer points are adjacent to the boundary. In Figure 5(a), we can also observe that the performance gap between $L = 0.1$ and $L = 10, 100$ widens then shrinks: If the truncation domain is small, not many samples are included in the truncation domain. Thus algorithms with all choices of L would suffer. However, as the truncation boundary grows, the difference starts to show: TruncSM with a smaller L has a better performance as we analyzed in Section 6.3. As V grows beyond a certain point, the dataset essentially becomes non-truncated, and TruncSM using large L reduces to a classic SM since \bar{g}_L are always capped at 1. At this time, TruncSM with all choices of L are consistent estimators of θ and we see TruncSM with different values of L converges to the same level of performance. Figure 5(b) shows a similar story but estimation error with different L converge to different levels as V enlarges: V never covers the center of our dataset thus estimators with different L never converge to the same level that would have achieved by the classic SM. Again TruncSM with a smaller L gives a better performance as we analyzed in Section 6.3.

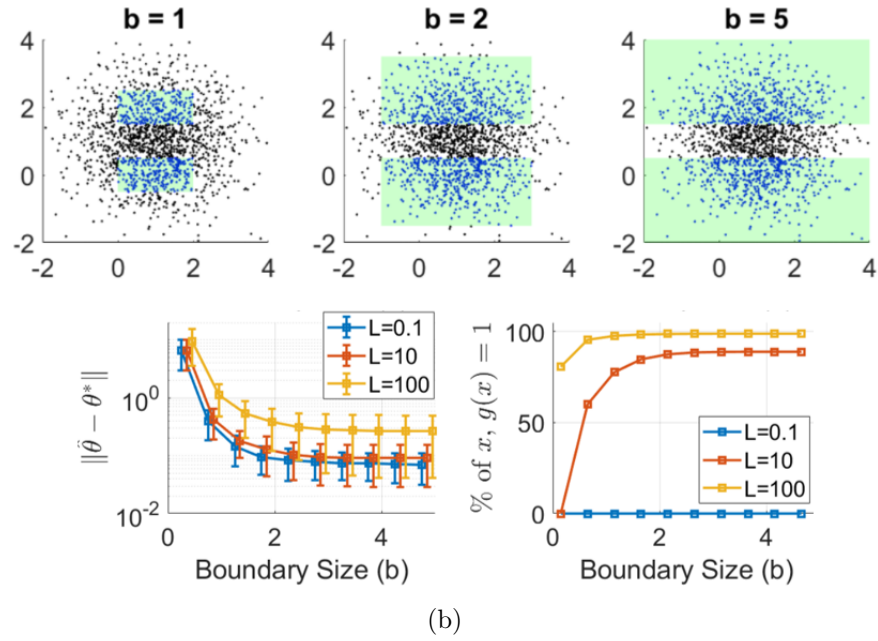
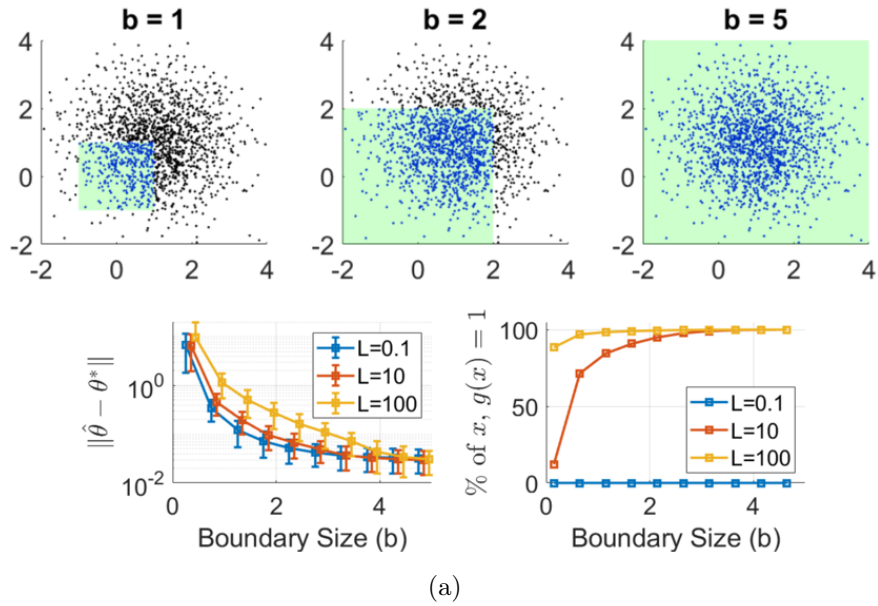


Figure 5: Performance of capped \bar{g}_L as V enlarges. b is the scaling multiplier of polygon vertices.

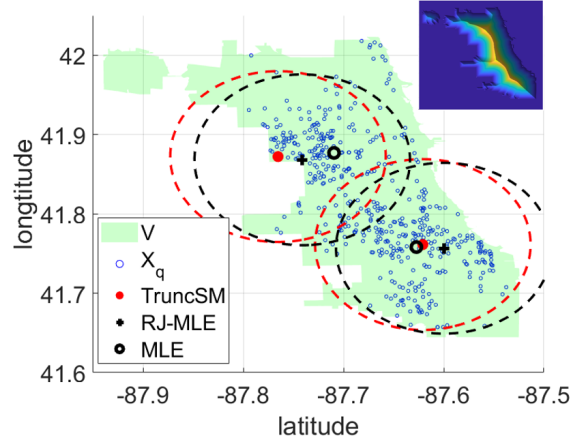


Figure 6: Chicago Crime dataset, whose truncation boundary is a polygon. Blue circles are homicide locations. g_0 is visualized at the upper right corner. The estimated component centers of TruncSM, RJ-MLE and MLE are plotted.

8.3 2008 Chicago Crime Dataset

We also test the performance of TruncSM on a real-world truncated density estimation problem: Analyzing the crime occurrences in Chicago. The dataset contains locations of homicides that happened in Chicago during 2008. We fit a Gaussian mixture model with two components on this dataset. The standard deviations of two components are fixed to the same value, which is chosen so that the 2-standard deviation radius of an individual Gaussian component can roughly cover the entire “width” of the city.

The estimated means of two components are plotted on Figure 6. The 2-standard deviation radius is plotted for TruncSM and RJ-MLE as red and black respectively. It can be seen that TruncSM, MLE and RJ-MLE all picked centers at the north and south side of the city. However, MLE picked a northern location inside of the city while TruncSM and RJ-MLE picked a location right next to the western border of Chicago.

In this case, TruncSM and RJ-MLE tend to put observed crimes on the decaying slope of a Gaussian density which would better explain the sudden truncation of observations at the west border and declining rate of crime from the west to the east. MLE, unaware of the truncation, puts the Gaussian center in the middle of the city, while clearly the crimes happen more rarely in the east.

Although all estimators tested in this section solve non-convex optimization problems, in the vast majority of runs with different initializations, we observe only very minor changes in terms of estimated Gaussian centers between different runs. See Appendix I for more discussion on this.

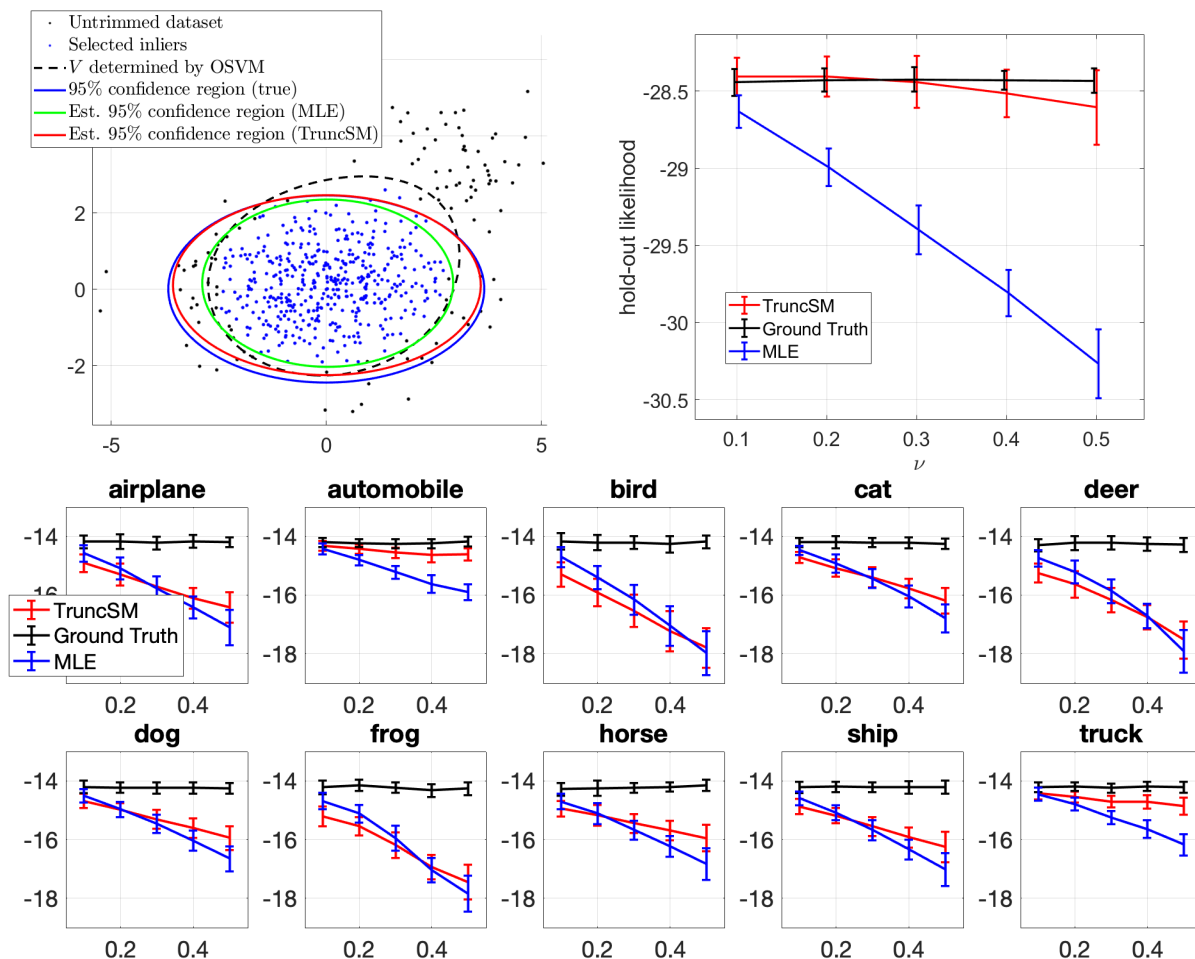


Figure 7: Top left: MLE underestimates the 95% confidence region due to the truncation. The confidence region estimated by TruncSM is much closer to the true confidence region. Top right, MLE getting less and less accurate as the percentage of truncated samples (controlled by ν) increases while TruncSM maintaining a good accuracy. Bottom row: TruncSM achieves a comparable or better performance than MLE as the percentage of truncation increases on CIFAR-10 dataset.

8.4 Outlier Over-trimming Compensation

Removing outliers is an important data preprocessing step. If we know the percentage of outliers in our dataset, we can adopt methods such as One-class Support Vector Machines (OSVM) [Schölkopf et al., 1999] to remove them. However, it is often impossible to determine the percentage of outliers a priori and setting the outlier percentage aggressively may result in inliers also being removed from the dataset.

Consider outlier trimming using OSVM. The method outputs a “decision function” $u(\mathbf{x}) := \sum_i \hat{\theta}_i \phi_i(\mathbf{x})$ which defines a domain $V := \{\mathbf{x} \in \mathbb{R}^d | u(\mathbf{x}) > 0\}$. OSVM chooses a V such that a certain proportion (say 80%) of our dataset is included in V . Then we discard any data point that is not in V as an outlier. However, if the specified outlier percentage is larger than it actually is, we will trim inliers from our dataset too, and our dataset become a truncated dataset. Estimation without considering the truncation boundary would lead to biased estimates.

This is demonstrated using the following simulated experiment. We sample

$$\mathbf{x}_{\text{inlier}} \sim \mathcal{N}\left(\mathbf{0}, \begin{bmatrix} 1.5^2 & 0 \\ 0 & 1 \end{bmatrix}\right), \quad \mathbf{x}_{\text{outlier}} \sim \mathcal{N}\left(\begin{bmatrix} 3.5 \\ 3 \end{bmatrix}, \begin{bmatrix} .8^2 & 0 \\ 0 & .8^2 \end{bmatrix}\right).$$

In total, 500 inlier samples and 50 outlier samples are drawn. The outlier percentage (ν) in OSVM is set to 20%. We use the trimmed dataset to estimate a truncated multivariate normal distribution $p_{\boldsymbol{\mu}, \boldsymbol{\Sigma}}(\mathbf{x}) \propto \mathcal{N}(\boldsymbol{\mu}, \boldsymbol{\Sigma})$, where $\boldsymbol{\Sigma}$ is restricted to be a diagonal matrix. The dataset (black dots), the selected inliers (blue dots) and the truncation domain V given by OSVM is visualized in the top left plot in Figure 7. In this section, g_0 and $\nabla_{\mathbf{x}} g_0$ are computed numerically using the constrained optimization described in Section 7.

On one hand, it can be seen that OSVM does separate the inliers from outliers using a boundary function $u(\mathbf{x})$. On the other hand, some inlier samples are also removed due to the aggressive setting of the outlier proportion. The vanilla MLE, without using the truncation information, underestimated the variance of the inlier distribution, while TruncSM accurately recovers the 95% confidence region using the estimated inlier density function. In this experiment, we use the Gaussian kernel for OSVM and allow MATLAB to automatically determine the kernel bandwidth according its predefined protocol. In the top right image of Figure 7, we perform the experiment in a much higher dimensional space: The inlier distribution is a 20 dimensional standard normal distribution while the outlier distribution is a 20 dimensional normal distribution with mean $\mathbf{1}$ and unit variance. Note in this experiment, the truncation boundary (induced by a kernel function) is highly irregular.

We plot the hold-out likelihood of MLE and TruncSM versus different settings of outlier proportion (ν) in OSVM. As we can see, the more aggressive the outlier trimming is, the worse the vanilla MLE performs. On the other hand, TruncSM only drops very slightly in performance as more and more data points are truncated.

We now perform an experiment on a real-world dataset CIFAR-10 which contains 10 different classes of 32 by 32 images. To speed up the computation, we reduced the dimension of the dataset to 10 using PCA. For each class, we artificially add 10% outliers that are drawn from a normal distribution with mean $\mathbf{1}$ and unit variance. We use both TruncSM and MLE

to estimate a multivariate Normal distribution for each class in the reduced 10 dimensional space and plot the hold-out likelihood of each method. The hold-out likelihood is plotted at the bottom row of Figure 7. For a large ν , we find that TruncSM performs better than MLE. The holdout likelihood shows that the estimation bias induced by the over-trimmed data can be indeed corrected by TruncSM. Although the advantage of TruncSM is smaller on this dataset, we argue that this is a very challenging problem: The dataset is hardly Gaussian so the model assumption used by TruncSM is wrong. Nonetheless, in some cases (automobile and truck), TruncSM significantly outperforms MLE.

9 Conclusion and Future Works

We propose an estimator for truncated statistical models with complex truncation boundaries based on generalized SM. The proposed method uses the distance (or capped distance) from data points to the truncation boundary as the weight function. Such a choice of weight function naturally arises from minimizing Stein Discrepancy and lowering the estimation error bound. The proposed weight function is also computationally favorable for high dimensional truncation domains. Experiments on synthetic data and the Chicago crime dataset show promising results. The proposed estimator was later applied to outlier trimming bias correction.

Although the proposed method achieves promising results in truncated density estimation, there are interesting open questions:

- How to choose an appropriate distance metric in g_0 ? For example, ℓ^1 and ℓ^2 distances are both valid choices for g_0 . Theorem 4 suggests that, in terms of upperbounding the statistical estimation error, the answer depends on q , ℓ_θ as well as V . However, how would the geometry of V , q and ℓ_θ affect the choice of the distance metric? See Appendix G for an empirical comparison between ℓ^1 and ℓ^2 distances.
- g_0 and \bar{g}_L come with hyperparameters: $\text{dist}(\cdot, \cdot)$ and L . Is there an efficient, numerical approach to determine these hyperparameters? Minimizing $\frac{F_g}{C_g}$ is a natural selection criterion, but it may be too computationally cumbersome.
- In many applications, our dataset is automatically filtered by algorithms. Outlier trimming by OSVM is just one example. Suppose we have mixed images of cats and dogs and a binary classifier, then we can easily identify high confidence region of each class. However, the classification step would also create artificial truncation boundaries around the distributions of individual classes. Can we use TruncSM to accurately reconstruct the true underlying distribution using these pre-classified images?

References

K. Atkinson and W. Han. *Theoretical numerical analysis*, volume 39. Springer, 2005.

- A. Barp, F-X. Briol, A. Duncan, M. Girolami, and L. Mackey. Minimum stein discrepancy estimators. In *Advances in Neural Information Processing Systems 32 (NIPS 2019)*, pages 12964–12976, 2019.
- W. Briec. Minimum distance to the complement of a convex set: Duality result. *Journal of Optimization Theory and Applications*, 93(2):301–319, 1997.
- K. Chwialkowski, H. Strathmann, and Arthur Gretton. A kernel test of goodness of fit. In *Proceedings of The 33rd International Conference on Machine Learning*, volume 48, pages 2606–2615, 2016.
- C. Daskalakis, T. Gouleakis, C. Tzamos, and M. Zampetakis. Efficient statistics, in high dimensions, from truncated samples. In *2018 IEEE 59th Annual Symposium on Foundations of Computer Science (FOCS)*, pages 639–649. IEEE, 2018.
- C. Daskalakis, T. Gouleakis, C. Tzamos, and M. Zampetakis. Computationally and statistically efficient truncated regression. In *Proceedings of the Thirty-Second Conference on Learning Theory*, volume 99, pages 955–960, 2019.
- L. C. Evans and R. F. Gariepy. *Measure Theory and Fine Properties of Functions*. CRC Press, Boca Raton, Florida, 1992.
- A. Hyvärinen. Estimation of non-normalized statistical models by score matching. *Journal of Machine Learning Research*, 6:695–709, 2005.
- A. Hyvärinen. Some extensions of score matching. *Computational statistics & data analysis*, 51(5):2499–2512, 2007.
- R. Kannan, L. Lovász, and M. Simonovits. Random walks and an $o^*(n^5)$ volume algorithm for convex bodies. *Random Structures & Algorithms*, 11(1):1–50, 1997.
- Q Liu, J. D. Lee, and M. Jordan. A kernelized stein discrepancy for goodness-of-fit tests. In *Proceedings of the 33rd International Conference on International Conference on Machine Learning*, pages 276–284, 2016.
- S. Lyu. Interpretation and generalization of score matching. In *Proceedings of the Twenty-Fifth Conference on Uncertainty in Artificial Intelligence*, pages 359–366. AUAI Press, 2009.
- K. Mardia, J. Kent, and A. Laha. Score matching estimators for directional distributions. *arXiv:1604.08470*, 2016.
- P. Milgrom and I. Segal. Envelope theorems for arbitrary choice sets. *Econometrica*, 70(2): 583–601, 2002.
- C. Moreira and J. de Uña-Álvarez. Kernel density estimation with doubly truncated data. *Electronic Journal of Statistics*, 6:501–521, 2012.

- B. Schölkopf, R. C. Williamson, A. J. Smola, J. Shawe-Taylor, and J. C Platt. Support vector method for novelty detection. In *Advances in Neural Information Processing Systems 12 (NIPS 1999)*, volume 12, pages 582–588, 1999.
- Bruce W. Turnbull. The empirical distribution function with arbitrarily grouped, censored and truncated data. *Journal of the Royal Statistical Society. Series B (Methodological)*, 38(3):290–295, 1976.
- A. W. van der Vaart. *Asymptotic Statistics*. Cambridge Series in Statistical and Probabilistic Mathematics. Cambridge University Press, 2000.
- S. Yu, M. Drton, and A. Shojaie. Generalized score matching for non-negative data. *Journal of Machine Learning Research*, 20(76):1–70, 2019.
- S. Yu, M. Drton, and A. Shojaie. Generalized score matching for general domains. *arXiv:2009.11428*, 2020.

A Generalized Score Matching

Assume that $p(\mathbf{x})$, $q(\mathbf{x})$ and $\mathbf{g}(\mathbf{x})$ take strictly positive values on the domain $V \subset \mathbb{R}^d$. Suppose that generalized SM objective function with weight \mathbf{g} is equal to zero, i.e.,

$$\mathbb{E}_q[\|\mathbf{g}^{1/2}(\mathbf{x}) \circ \nabla_{\mathbf{x}} \log p(\mathbf{x}) - \mathbf{g}^{1/2}(\mathbf{x}) \circ \nabla_{\mathbf{x}} \log q(\mathbf{x})\|^2] = 0. \quad (\text{A.16})$$

Then, we have $\nabla_{\mathbf{x}}(\log p(\mathbf{x}) - \log q(\mathbf{x})) = \mathbf{0}$, meaning that $p(\mathbf{x}) = Cq(\mathbf{x})$ on (the connected domain) V with a positive constant C . Since both p and q are the probability densities on V , we have $C = 1$.

B Proof of Theorem 2

Proof. In this proof, we apply Theorem 1 to derive a tractable expression for $M(\boldsymbol{\theta})$. Let us consider the second term of $M(\boldsymbol{\theta})$. As $q(\mathbf{x})$ and $g_k(\mathbf{x})\partial_k \log p_{\boldsymbol{\theta}}(\mathbf{x})$ are functions in the Sobolev-Hilbert space of the first order, the direct application of Theorem 1 leads to

$$\begin{aligned} & \sum_{k=1}^d \int_V g_k(\mathbf{x}) [\partial_k \log p_{\boldsymbol{\theta}}(\mathbf{x})] [\partial_k \log q(\mathbf{x})] q(\mathbf{x}) d\mathbf{x} \\ &= \sum_{k=1}^d \int_V g_k(\mathbf{x}) [\partial_k \log p_{\boldsymbol{\theta}}(\mathbf{x})] [\partial_k q(\mathbf{x})] d\mathbf{x} \\ &= \sum_{k=1}^d \left\{ \int_{\partial V} g_k(\mathbf{x}) [\partial_k \log p_{\boldsymbol{\theta}}(\mathbf{x})] q(\mathbf{x}) \nu_k(\mathbf{x}) ds - \int_V \partial_k [g_k(\mathbf{x}) \partial_k \log p_{\boldsymbol{\theta}}(\mathbf{x})] q(\mathbf{x}) d\mathbf{x} \right\} \\ &= - \sum_{k=1}^d \int_V \partial_k [g_k(\mathbf{x}) \partial_k \log p_{\boldsymbol{\theta}}(\mathbf{x})] q(\mathbf{x}) d\mathbf{x}. \end{aligned}$$

The second equality is ensured by Theorem 1 and the third equality holds from the boundary condition assumed in the theorem. \square

C Proofs of Theorem 3 and Corollary 1 in Section 5

C.1 Proof of Lemma 3

$$\max_{g_k \in \text{Lip}_0^L(V)} \mathbb{E}_q \left[\sum_k (\partial_k \ell_{\boldsymbol{\theta}} - \partial_k \log q)^2 g_k \right] = L \cdot \mathbb{E}_q \left[\sum_k (\partial_k \ell_{\boldsymbol{\theta}} - \partial_k \log q)^2 g_0 \right] = L \cdot \text{FH}_{g_0}(q, p_{\boldsymbol{\theta}}),$$

The first equality holds since $\forall k, (\partial_k \ell_{\boldsymbol{\theta}} - \partial_k \log q)^2 \geq 0$. Since for all $g_k \in \text{Lip}_0^L(V)$, $g_k(\mathbf{z}) = 0, \forall \mathbf{z} \in \partial V$,

$$g_k(\mathbf{x}) = g_k(\mathbf{x}) - g_k(\mathbf{x}') \leq Ld(\mathbf{x}, \mathbf{x}'), \forall \mathbf{x}' \in \partial V \implies g_k(\mathbf{x}) \leq L \cdot \min_{\mathbf{z} \in \partial V} d(\mathbf{x}, \mathbf{z}) = Lg_0(\mathbf{x}), \quad (\text{C.17})$$

Hence the second equality.

C.2 Proofs of Theorem 3

Proof. As we stated in the proof of v Lemma 2, due to Rademacher's theorem [Evans and Gariepy, 1992], any Lipschitz function defined on a Lipschitz domain is in $H^1(V)$, hence $g_k \in H^1(V)$ and $\forall k, f_k \in H^1(V)$. Using the fact that $f_k, q, \ell_\theta \in H^1(V)$, $f_k(\mathbf{x}) = 0, \forall \mathbf{x} \in \partial V$, we can verify that \mathbf{f} is in a Stein class of q by applying the same integration by parts techniques used in Section B. Therefore, we can write the Stein discrepancy between p_θ and q as:

$$\max_{\mathbf{f} \in \mathcal{F}} \mathbb{E}_q [T_{p_\theta} \mathbf{f}] = \max_{\mathbf{f} \in \mathcal{F}} \mathbb{E}_q [T_{p_\theta} \mathbf{f} - T_q \mathbf{f}]. \quad (\text{C.18})$$

Now we optimize (C.18) analytically using Theorem 2 in Barp et al. [2019]

$$\begin{aligned} \max_{\mathbf{f} \in \mathcal{F}} \mathbb{E}_q [T_{p_\theta} \mathbf{f} - T_q \mathbf{f}] &= \max_{g_k \in \text{Lip}_0^L(V)} \max_{\mathbf{h}} \mathbb{E}_q \left[\sum_k (\partial_k \ell_\theta - \partial_k \log q) \cdot g_k^{\frac{1}{2}} h_k \right] \\ &= \max_{g_k \in \text{Lip}_0^L(V)} \sqrt{\mathbb{E}_q \left[\sum_k (\partial_k \ell_\theta - \partial_k \log q)^2 g_k \right]}. \end{aligned}$$

Applying Lemma 3, we obtain the desired result. \square

C.3 Proof of Corollary 1

Proof. The proof is mostly the same as the proof of Theorem 3. However we need to prove a different version of Lemma 3 for the capped $\text{Lip}_0^L(V)$ family.

Lemma 3 states $g_k(\mathbf{x}) \leq L \cdot \min_{\mathbf{z} \in \partial V} \text{dist}(\mathbf{x}, \mathbf{z}) = g_0(\mathbf{x})$ for all $g_k \in \text{Lip}_0^L(V)$. Further, we know that $g_k \leq 1$ by definition. Therefore $g_k(\mathbf{x}) \leq \min(1, Lg_0(\mathbf{x})) = \bar{g}_L$. Notice that $\bar{g}_L \in \overline{\text{Lip}}_0^L(V)$. Using the same argument in Section C.1, we can see

$$\max_{g_k \in \overline{\text{Lip}}_0^L(V)} \mathbb{E}_q \left[\sum_k (\partial_k \ell_\theta - \partial_k \log q)^2 g_k \right] = \text{FH}_{\bar{g}_L}(q, p_\theta).$$

Applying this result to the last step in Section C.2, gives the desired result. \square

D Proof of Theorem 4

D.1 Proof of Theorem 4

We assume that

$$\mathbb{E} \left[\sup_{\theta: \|\theta - \theta^*\| \leq \delta} |\mathbb{G}_n(m_\theta - m_{\theta^*})| \right] \leq C'_g \delta^\beta, \quad (\text{D.19})$$

where $\mathbb{G}_n f = \frac{1}{\sqrt{n}} \sum_{i=1}^n (f(X_i) - \mathbb{E}_q[f(X)])$ for the independent random variables X_1, \dots, X_n from q , and C'_g is a positive constant depending on the function g satisfying the same property as C_g . Then, the estimation accuracy is given by the following theorem.

Theorem D.5 (Theorem 5.52 in [van der Vaart \[2000\]](#)). *Suppose Assumption 1, 2 and (D.19) hold for $\alpha > \beta > 0$ and $\alpha > 1$. Then, for any positive integer K we have*

$$P \left\{ \|\hat{\boldsymbol{\theta}} - \boldsymbol{\theta}^*\| > \frac{2^K}{n^{1/(2(\alpha-\beta))}} \right\} \leq 2^{K(\beta-\alpha)} \frac{2^{2\alpha}}{2^{\alpha-1} - 1} \frac{C'_g}{C_g}.$$

Hence, we have $\|\hat{\boldsymbol{\theta}} - \boldsymbol{\theta}^*\| = O_p(n^{-1/(2(\alpha-\beta))})$. Our concern is the relation between the coefficient of the convergence rate and the weight function g .

The upper bound of the expectation (D.19) is closely related to the covering number of the parameter space $\Theta \subset \mathbb{R}^r$. Let us define $N_{[]}(\varepsilon, \mathcal{F}, L^2(Q))$ be the bracketing number of \mathcal{F} with the radius ε under the norm of $L^2(Q)$ and $J_{[]}(\delta, \mathcal{F}, L^2(Q))$ be

$$J_{[]}(\delta, \mathcal{F}, L^2(Q)) = \int_0^\delta \sqrt{\log N_{[]}(\varepsilon, \mathcal{F}, L^2(Q))} d\varepsilon$$

Then, the following theorem holds.

Theorem D.6 (Corollary 19.35 of [van der Vaart \[2000\]](#)). *Let F be an envelope for the function class $\mathcal{F} \subset L^2(Q)$, i.e., $\sup_{f \in \mathcal{F}} \|f(\mathbf{x})\|_\infty \leq F(\mathbf{x})$ for every $\mathbf{x} \in V$ and suppose $\mathbb{E}_Q[|F(X)|^2] < \infty$. Then, we have*

$$\mathbb{E} \left[\sup_{f \in \mathcal{F}} |\mathbb{G}_n(f)| \right] \leq C J_{[]}(\|F\|_{L^2(Q)}, \mathcal{F}, L^2(Q)),$$

where C is a universal constant.

The bracketing number of the parametric model is given by the following proposition.

Proposition 2 (Example 19.6 in [van der Vaart \[2000\]](#)). *The bracketing number of the parametrized loss function $m_{\boldsymbol{\theta}}(\mathbf{x})$ is given as follows. Let $\Theta \subset \mathbb{R}^r$ be contained in a ball of radius R . Let $\mathcal{F} = \{m_{\boldsymbol{\theta}}(\mathbf{x}) \mid \boldsymbol{\theta} \in \Theta\}$ be a function class indexed by Θ . Suppose there exists a function $\dot{m}(\mathbf{x})$ with $\|\dot{m}\|_{L^2(Q)} < \infty$ such that*

$$|m_{\boldsymbol{\theta}_1}(\mathbf{x}) - m_{\boldsymbol{\theta}_2}(\mathbf{x})| \leq \dot{m}(\mathbf{x}) \|\boldsymbol{\theta}_1 - \boldsymbol{\theta}_2\|_2$$

for all $\mathbf{x} \in V$ and $\boldsymbol{\theta}_1, \boldsymbol{\theta}_2 \in \Theta$. Then, for every $\varepsilon > 0$,

$$N_{[]}(\varepsilon \|\dot{m}\|_{L^2(Q)}, \mathcal{F}, L^2(Q)) \leq \left(1 + \frac{4R}{\varepsilon}\right)^r.$$

In our case, we need to evaluate $\mathbb{E}[\sup_{f \in \mathcal{F}_\delta} |\mathbb{G}_n(f)|]$ for

$$\mathcal{F}_\delta := \{m_{\boldsymbol{\theta}}(\mathbf{x}) - m_{\boldsymbol{\theta}^*}(\mathbf{x}) \mid \boldsymbol{\theta} \in \Theta, \|\boldsymbol{\theta} - \boldsymbol{\theta}^*\| \leq \delta\},$$

where $\boldsymbol{\theta}^*$ is the minimizer of the expected loss $M(\boldsymbol{\theta})$. The function $\dot{m}(\mathbf{x})$ in Proposition 2 should satisfy

$$|(m_{\boldsymbol{\theta}_1}(\mathbf{x}) - m_{\boldsymbol{\theta}^*}(\mathbf{x})) - (m_{\boldsymbol{\theta}_2}(\mathbf{x}) - m_{\boldsymbol{\theta}^*}(\mathbf{x}))| = |m_{\boldsymbol{\theta}_1}(\mathbf{x}) - m_{\boldsymbol{\theta}_2}(\mathbf{x})| \leq \dot{m}(\mathbf{x}) \|\boldsymbol{\theta}_1 - \boldsymbol{\theta}_2\|.$$

Then, Proposition 2 leads to

$$N_{\square}(\varepsilon \|\dot{m}\|_{L^2(Q)}, \mathcal{F}_\delta, L^2(Q)) \leq \left(1 + \frac{4\delta}{\varepsilon}\right)^r.$$

The envelope function $F_\delta(\mathbf{x})$ of \mathcal{F}_δ is given by $F_\delta(\mathbf{x}) = \dot{m}(\mathbf{x})\delta$, because

$$|m_{\boldsymbol{\theta}}(\mathbf{x}) - m_{\boldsymbol{\theta}^*}(\mathbf{x})| \leq \dot{m}(\mathbf{x}) \|\boldsymbol{\theta} - \boldsymbol{\theta}^*\| \leq \dot{m}(\mathbf{x})\delta.$$

Hence, we obtain

$$N_{\square}(\varepsilon \|F_\delta\|_{L^2(Q)}, \mathcal{F}_\delta, L^2(Q)) = N_{\square}(\varepsilon\delta \|\dot{m}\|_{L^2(Q)}, \mathcal{F}_\delta, L^2(Q)) \leq \left(1 + \frac{4}{\varepsilon}\right)^r,$$

and thus,

$$\mathbb{E}[\sup_{f \in \mathcal{F}_\delta} |\mathbb{G}_n(f)|] \leq C\delta \|\dot{m}\|_{L^2(Q)} \sqrt{r} \int_0^1 \sqrt{\log\left(1 + \frac{4}{\varepsilon}\right)} d\varepsilon \leq C' \sqrt{r}\delta \|\dot{m}\|_{L^2(Q)}$$

holds, where C and C' are universal constants. We find that β in (D.19) is given by $\beta = 1$.

Let us evaluate the norm $\|\dot{m}\|_{L^2(Q)}$. For the function A_k and B_k in (8), we have the following inequalities

$$\begin{aligned} |A_k(\mathbf{x}, \boldsymbol{\theta}_1) - A_k(\mathbf{x}, \boldsymbol{\theta}_2)| &\leq \dot{A}_k(\mathbf{x}) \|\boldsymbol{\theta}_1 - \boldsymbol{\theta}_2\|, \\ |B_k(\mathbf{x}, \boldsymbol{\theta}_1) - B_k(\mathbf{x}, \boldsymbol{\theta}_2)| &\leq \dot{B}_k(\mathbf{x}) \|\boldsymbol{\theta}_1 - \boldsymbol{\theta}_2\|. \end{aligned} \quad (\text{D.20})$$

It is straightforward to see that the following \dot{m} satisfies the required condition:

$$\dot{m}(\mathbf{x}) = \sum_k \{g_k(\mathbf{x}) \dot{A}_k(\mathbf{x}) + |\partial_k g_k(\mathbf{x})| \dot{B}_k(\mathbf{x})\}.$$

Cauchy-Schwarz inequality leads to $\|g_k \dot{A}_k\|_{L^2(Q)} \leq (\mathbb{E}_q[\dot{A}_k^4])^{1/4} (\mathbb{E}_q[g_k^4])^{1/4}$. The similar inequality holds for $\|\dot{B}_k \partial_k g_k\|_{L^2(Q)}$. Hence, we have

$$\|\dot{m}\|_{L^2(Q)} \leq \Gamma(\mathbf{g}; A, B) := \sum_{k=1}^d \left\{ (\mathbb{E}_q[\dot{A}_k^4] \mathbb{E}_q[g_k^4])^{1/4} + (\mathbb{E}_q[\dot{B}_k^4] \mathbb{E}_q[|\partial_k g_k|^4])^{1/4} \right\}. \quad (\text{D.21})$$

In summary, we have the estimation error bound in Theorem 4.

E Some More Analysis of Weight Functions

In this subsection, we also assume that the statistical model is realizable, i.e., $q = p_{\theta^*}$ holds. Let U be a subset in the domain V . Under the regularity condition later shown in Appendix E.1, one can find that the constant $C_{\mathbf{g}}$ in (9) is given by

$$C_{\mathbf{g}} = \min_{\mathbf{x} \in U} \min_{k \in [d]} g_k(\mathbf{x}) \quad (\text{E.22})$$

up to a constant independent of \mathbf{g} . As the continuous and non-negative weight function $g_k(\mathbf{x})$ can take zero only on the boundary ∂V , $C_{\mathbf{g}} > 0$ holds if U is a closed subset which does not include boundary points of V .

Let us consider $\Gamma(\mathbf{g}; A, B)/C_{\mathbf{g}}$ in the upper bound in Theorem 4. The following theorem ensures that the minimum function

$$h(\mathbf{x}) = \min_{k \in [d]} g_k(\mathbf{x}) \quad (\text{E.23})$$

improves the upper bound of the estimation error under some conditions on g_k .

Theorem E.7. *Let $\mathbf{g} = (g_1, \dots, g_d)$ and $\mathbf{h} = (h, \dots, h)$ be the weight functions, where h is defined by (E.23). Suppose that g_k is differentiable on V except a measure zero set and that the set $\{\mathbf{x} \in V \mid g_k(\mathbf{x}) = g_{k'}(\mathbf{x}), \exists k, k' \in [d], k \neq k'\}$ is measure zero. We assume that*

$$|\partial_k g_k(\mathbf{x})| \geq |\partial_k g_{k^*}(\mathbf{x})|,$$

holds for $\mathbf{x} \in V$ and $k \in [d]$, where $k^* \in [d]$ is the number such that $h(\mathbf{x}) = g_{k^*}(\mathbf{x})$. Then, we have

$$\frac{\Gamma(\mathbf{h}; A, B)}{C_{\mathbf{h}}} \leq \frac{\Gamma(\mathbf{g}; A, B)}{C_{\mathbf{g}}},$$

where $C_{\mathbf{g}}$ and $C_{\mathbf{h}}$ are defined by (E.22).

The proof is found in Appendix E.2.

Example 2 (Bounded Rectangular Domain). *For the d -dimensional rectangular $V = \prod_{k=1}^d [0, c_k]$, let us consider the statistical accuracy of the generalized score matching (SM) method [Yu et al., 2019] with $g_k(\mathbf{x}) = \min\{x_k, c_k - x_k\}$, and $h(\mathbf{x}) = \min_k g_k(\mathbf{x})$. Note that the weight h is nothing but g_0 in (5). According to Theorem E.7, we find that the estimator with the weight h is superior to the estimator with the above g_1, \dots, g_d in the sense of the estimation error bound.*

Example 3 (Unit ball under p -norm). *Let us define V as the d -dimensional unit ball under p -norm, $V = \{\mathbf{x} \in \mathbb{R}^d \mid \|\mathbf{x}\|_p \leq 1\}$. The weight $g_k(\mathbf{x})$ is defined by the distance from \mathbf{x} to the boundary of V along the k -th axis. This is expressed by*

$$g_k(\mathbf{x}) = \max\{|\varepsilon| \mid \mathbf{x} + \varepsilon \mathbf{e}_k \in V\} = \min\{(1 - \|\mathbf{x}_{(k)}\|_p^p)^{1/p} - x_k, x_k + (1 - \|\mathbf{x}_{(k)}\|_p^p)^{1/p}\},$$

where \mathbf{e}_k is the unit vector along with the k -th axis, $\mathbf{x}_{(k)}$ is the $d-1$ dimensional vector dropped the k -th element x_k from \mathbf{x} . Some calculation yields the inequality $|\partial_k g_k(\mathbf{x})| = 1 \geq |\partial_k g_\ell(\mathbf{x})|$ for $\ell = \underset{k}{\operatorname{argmin}} g_k(\mathbf{x})$. Hence, the minimum function $h(\mathbf{x}) = \min_k g_k(\mathbf{x})$ improves the error bound of the estimator with the weight g_k . One can confirm that $h(\mathbf{x}) = \min_{\mathbf{z} \in \partial V} \|\mathbf{x} - \mathbf{z}\|_1$ holds. Likewise, for the truncated domain $V = \{\mathbf{x} = (x_1, \dots, x_d) \in \mathbb{R}^d \mid \|\mathbf{x}\|_p \leq 1, x_i \geq c_i\}$, $c_i \in \mathbb{R}$, one can prove the inequality $|\partial_k g_k(\mathbf{x})| = 1 \geq |\partial_k g_\ell(\mathbf{x})|$. The above assertions are explained in Appendix E.3.

Under the assumption of Theorem E.7, we find that the homogeneous weight \mathbf{h} improves the upper bound of the estimation error for the estimator with \mathbf{g} . Furthermore, the weight \mathbf{h} corresponds to the minimum ℓ^1 distance to the boundary as shown in Example 3. To compare the distance-based homogeneous weights, we need to evaluate the upper bound for each distance. In Appendix G, we show numerical comparison between ℓ^1 and ℓ^2 distances and numerical evaluation of the theoretical upper bound.

E.1 Derivation of (E.22)

Suppose the true probability $q(\mathbf{x})$ is $p_{\boldsymbol{\theta}^*}(\mathbf{x})$. Let U be an open subset of V . Then, we have

$$\begin{aligned} M(\boldsymbol{\theta}) - M(\boldsymbol{\theta}^*) &= \int_V \sum_k g_k(\mathbf{x}) (\partial_k \log p_{\boldsymbol{\theta}}(\mathbf{x}) - \partial_k \log p_{\boldsymbol{\theta}^*}(\mathbf{x}))^2 p_{\boldsymbol{\theta}^*}(\mathbf{x}) d\mathbf{x} \\ &\geq \int_U \sum_k g_k(\mathbf{x}) (\partial_k \log p_{\boldsymbol{\theta}}(\mathbf{x}) - \partial_k \log p_{\boldsymbol{\theta}^*}(\mathbf{x}))^2 p_{\boldsymbol{\theta}^*}(\mathbf{x}) d\mathbf{x} \\ &\geq \min_{\mathbf{x} \in U} \min_k \{g_k(\mathbf{x})\} \int_U \sum_k (\partial_k \log p_{\boldsymbol{\theta}}(\mathbf{x}) - \partial_k \log p_{\boldsymbol{\theta}^*}(\mathbf{x}))^2 p_{\boldsymbol{\theta}^*}(\mathbf{x}) d\mathbf{x}. \end{aligned}$$

Suppose that the Hessian matrix of

$$\int_U \sum_k (\partial_k \log p_{\boldsymbol{\theta}}(\mathbf{x}) - \partial_k \log p_{\boldsymbol{\theta}^*}(\mathbf{x}))^2 p_{\boldsymbol{\theta}^*}(\mathbf{x}) d\mathbf{x} \quad (\text{E.24})$$

as the function of $\boldsymbol{\theta}$ is non-degenerate, there exists a constant C_0 independent of \mathbf{g} such that the above integral is bounded below by $C_0 \|\boldsymbol{\theta} - \boldsymbol{\theta}^*\|^2$. Hence, $C_{\mathbf{g}} = \min_{\mathbf{x} \in U} \min_k \{g_k(\mathbf{x})\}$ satisfies the required condition.

E.2 Proof of Theorem E.7

From the definition of h , one can find

$$C_{\mathbf{g}} = \min_{\mathbf{x} \in U} \min_k g_k(\mathbf{x}) = \min_{\mathbf{x} \in U} h(\mathbf{x}) = C_{\mathbf{h}}.$$

We evaluate $\Gamma(\mathbf{g}; A, B)$ and $\Gamma(\mathbf{h}; A, B)$. As for the derivative function, the assumption guarantees that $\partial_k h(\mathbf{x}) = \partial_k g_{k^*}(\mathbf{x})$ and $|\partial_k g_k(\mathbf{x})| \geq |\partial_k g_{k^*}(\mathbf{x})|$. Hence, we have

$$\begin{aligned}\Gamma(\mathbf{g}; A, B) &= \sum_{k=1}^d (\mathbb{E}_q[\dot{A}_k^4] \mathbb{E}_q[g_k^4])^{1/4} + \sum_{k=1}^d (\mathbb{E}_q[\dot{B}_k^4] \mathbb{E}_q[|\partial_k g_k|^4])^{1/4} \\ &\geq \sum_{k=1}^d (\mathbb{E}_q[\dot{A}_k^4] \mathbb{E}_q[(\min_k g_k)^4])^{1/4} + \sum_{k=1}^d (\mathbb{E}_q[\dot{B}_k^4] \mathbb{E}_q[|\partial_k g_{k^*}|^4])^{1/4} \\ &= \Gamma(\mathbf{h}; A, B).\end{aligned}$$

As a result, we obtain $\frac{\Gamma(\mathbf{g}; A, B)}{C_g} \geq \frac{\Gamma(\mathbf{h}; A, B)}{C_h}$.

E.3 Some Equations in Example 3

Proof of $|\partial_k g_k(\mathbf{x})| \geq |\partial_k g_{k^*}(\mathbf{x})|$: Without loss of generality, we suppose $\mathbf{x} = (x_1, \dots, x_d) \geq \mathbf{0}$. Then, $g_k(\mathbf{x}) = (1 - \|\mathbf{x}_{(k)}\|_p^p)^{1/p} - x_k$ holds. Firstly, we prove that $g_\ell(\mathbf{x}) < g_k(\mathbf{x})$ leads to $x_k < x_\ell$. For the sake of simplicity let us assume $k = 1$ and $\ell = 2$. Let us define $c^p = 1 - x_3^p - \dots - x_d^p$ for $c \geq 0$. Then, we find that $g_2(\mathbf{x}) < g_1(\mathbf{x})$ leads to $(c^p - x_1^p)^{1/p} + x_1 < (c^p - x_2^p)^{1/p} + x_2$. The function $f(x) = (c^p - x^p)^{1/p} + x$ for $0 \leq x \leq c$ is concave, takes the maximum value at $x = c/2^{1/p} (< c)$ and satisfies $f(x) = f((c^p - x^p)^{1/p})$. When y lies on the interval between x and $(c^p - x^p)^{1/p}$, $f(x) = f((c^p - x^p)^{1/p}) \leq f(y)$ holds. Suppose $x_1^p + x_2^p \leq c^2$ and $f(x_1) < f(x_2) = f((c^p - x_2^p)^{1/p})$. If x_1 lies on the interval between x_2 and $(c^p - x_2^p)^{1/p}$, $f(x_2) \leq f(x_1)$ holds and it is the contradiction. Hence we have $x_1 < x_2$. Next, we evaluate the absolute value of the derivatives. When $g_\ell(\mathbf{x}) < g_k(\mathbf{x})$, $x_k < x_\ell$ holds. For $k \neq \ell$, we obtain $|\partial_k g_k(\mathbf{x})| = 1$ and $|\partial_k g_\ell(\mathbf{x})| = |x_k|^{p-1} (1 - \|\mathbf{x}_{(\ell)}\|_p^p)^{1/p-1} \leq |x_\ell|^{p-1} (|x_\ell|^p)^{1/p-1} = 1$ for $p \geq 1$.

Rough sketch of the proof of $h(\mathbf{x}) = \min_{z \in \partial V} \|\mathbf{x} - z\|_1$: Suppose that all the vertexes of the polytope $B_1(\mathbf{x}, c) := \{z \in \mathbb{R}^d \mid \|\mathbf{x} - z\|_1 \leq c\}$ are included in V . Then, $B_1(\mathbf{x}, c) \subset V$ holds as V is convex. Clearly, $h(\mathbf{x})$ is expressed by $\sup_{c \geq 0} \{c \mid B_1(\mathbf{x}, c) \subset V\}$. This is nothing but the ℓ^1 -distance from \mathbf{x} to the boundary of V .

F Derivation of (13)

Let us define U by $U = \{\mathbf{x} \in V \mid g_0(\mathbf{x}) \geq c\}$. We see that $\min_{\mathbf{x} \in U} \bar{g}_L(\mathbf{x}) = 1$ holds from Section E.1. Hence we have $C_{\bar{g}_L} = 1$. Let us evaluate the fourth order moments of \bar{g}_L :

$$\begin{aligned}\mathbb{E}[\bar{g}_L^4] &= L^4 \int_0^{1/L} z^4 p_{\text{dist}}(z) dz + \int_{z \geq 1/L} p_{\text{dist}}(z) dz \\ &= L^4 \int_0^{1/L} z^4 p_{\text{dist}}(z) dz + 1 - \int_0^{1/L} p_{\text{dist}}(z) dz = 1 - \frac{C}{L^{1+\beta}},\end{aligned}$$

where C is a positive constant such as $c_{b,\beta} := \frac{4b}{\beta^2+6\beta+5} \leq C \leq C_{b',\beta} := \frac{4b'}{\beta^2+6\beta+5}$. Due to the non-negativity of $\mathbb{E}[\bar{g}_L^4]$, $L^{1+\beta} \geq C$ should hold. This inequality is guaranteed from $1 \geq \int_0^{1/L} b'z^\beta dz \geq \int_0^{1/L} p_{\text{dist}}(z)dz$. Let us evaluate the second term of $\Gamma(\mathbf{g}; A, B)$. The derivative $\partial_k \bar{g}_L$ is given by

$$\partial_k \bar{g}_L(\mathbf{x}) = \begin{cases} L \frac{x_k - \tilde{x}_k}{\|\mathbf{x} - \tilde{\mathbf{x}}\|}, & g_0(\mathbf{x}) < 1/L, \\ 0, & g_0(\mathbf{x}) > 1/L, \end{cases}$$

where $\tilde{\mathbf{x}}$ is the minimum solution of $\min_{\mathbf{z} \in \partial V} \|\mathbf{x} - \mathbf{z}\|$. Hence, we have

$$\mathbb{E}[|\partial_k \bar{g}_L|^4] = L^4 \int_{g_0(\mathbf{x}) \leq 1/L} \frac{|x_k - \tilde{x}_k|^4}{g_0(\mathbf{x})^4} q(\mathbf{x}) d\mathbf{x} \leq L^4 \int_0^{1/L} p_{\text{dist}}(z) dz \leq \frac{b'}{\beta+1} L^{-\beta+3}.$$

Next, we evaluate the lower bound of the fourth moment of the derivative $\partial_k g_k$. Jensen's inequality yields that

$$\begin{aligned} \mathbb{E}[|\partial_k \bar{g}_L|^4] &= L^4 \sum_{k=1}^d \int_{g_0(\mathbf{x}) \leq 1/L} \frac{|x_k - \tilde{x}_k|^4}{g_0(\mathbf{x})^4} q(\mathbf{x}) d\mathbf{x} \\ &\geq dL^4 \left(\frac{1}{d} \sum_{k=1}^d \int_{g_0(\mathbf{x}) \leq 1/L} \frac{|x_k - \tilde{x}_k|^2}{g_0(\mathbf{x})^2} q(\mathbf{x}) d\mathbf{x} \right)^2 \\ &= \frac{L^4}{d} \left(\int_{g_0(\mathbf{x}) \leq 1/L} q(\mathbf{x}) d\mathbf{x} \right)^2 \geq \frac{b^2}{d(\beta+1)^2} L^{2(1-\beta)} \end{aligned}$$

Let us define $C_A = \sum_{k=1}^d (\mathbb{E}_q[\dot{A}_k^4])^{1/4}$, $C_B = \sum_{k=1}^d (\mathbb{E}_q[\dot{B}_k^4])^{1/4}$, $c_0 = (b^2/(d(\beta+1)^2))^{1/4}$, and $c_1 = (b'/(\beta+1))^{1/4}$. Then, we have

$$C_A \left(1 - \frac{C_{b',\beta}}{L^{\beta+1}}\right)^{1/4} + C_B c_0 L^{(1-\beta)/2} \leq \frac{\Gamma(\bar{g}_L; A, B)}{C_{\bar{g}_L}} \leq C_A \left(1 - \frac{c_{b,\beta}}{L^{\beta+1}}\right)^{1/4} + C_B c_1 L^{(3-\beta)/4}.$$

G Choice of Weight Function: ℓ^1 vs. ℓ^2 distance

Table 1: Comparison of the weight h_p , $p = 1, 2$. The table shows $\{Rd\mathbb{E}_q[|h_p|^4]^{1/4} + (1-R) \sum_{k=1}^d \mathbb{E}_q[|\partial_k h_p|^4]^{1/4}\}/C_{h_p}$ for $R = 0.2, 0.8$.

weight \ dim	R = 0.2					R = 0.8				
	2	3	4	5	6	2	3	4	5	6
h_1	3.160	4.558	5.939	7.309	8.685	1.569	2.088	2.537	2.975	3.371
h_2	3.073	4.279	5.412	6.496	7.552	1.545	2.012	2.402	2.764	3.081

In this section, we test different metrics for g_0 : ℓ^1 distance $\text{dist}(\mathbf{x}, \mathbf{y}) := \|\mathbf{x} - \mathbf{y}\|_1$ and ℓ^2 distance $\text{dist}(\mathbf{x}, \mathbf{y}) := \|\mathbf{x} - \mathbf{y}\|_2$. The dataset is generated from $\mathcal{N}(\mathbf{1}_d \cdot 0.5, \mathbf{I}_d)$, where $\mathbf{1}_d$

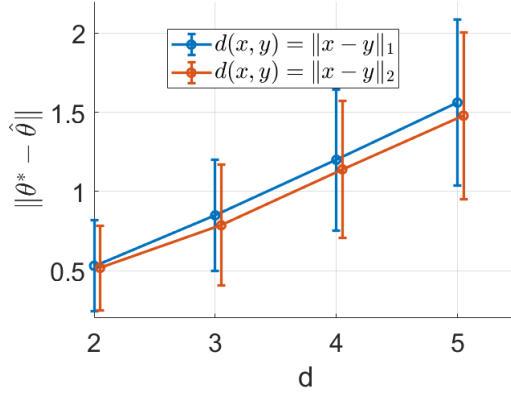


Figure 8: Estimation accuracy of TruncSM using ℓ^1 vs. ℓ^2 distance.

and \mathbf{I}_d are the d dimensional all one vector and the $d \times d$ identity matrix respectively. The truncation domain is $V = \{\mathbf{x} \mid \|\mathbf{x}\|_1 < 1 \text{ and } x_d > 0\}$. 150 samples are generated. We plot the estimation error $\|\hat{\boldsymbol{\theta}} - \boldsymbol{\theta}^*\|$ and its standard deviation for both choices of distances: ℓ^1 and ℓ^2 versus the dimensionality d in Figure 8. It can be seen that the Euclidean distance, i.e., ℓ^2 distance consistently achieves slightly lower error than the ℓ^1 distance.

Let us numerically evaluate the upper bound $\Gamma(\mathbf{h}_p; A, B)/C_{\mathbf{h}_p}$ for the weight $\mathbf{h}_p = (h_p, \dots, h_p)$, where $h_p(\mathbf{x}) = \min_{\mathbf{z} \in \partial V} \|\mathbf{x} - \mathbf{z}\|_p$, $p = 1, 2$. Let “sup $_U$ ” be the supremum over all open subsets of V . Then, we have $\sup_U \min_{\mathbf{x} \in U} h_1(\mathbf{x}) = 1/2$ and $\sup_U \min_{\mathbf{x} \in U} h_2(\mathbf{x}) = 1/(\sqrt{d} + 1)$. In order to obtain the tight bound, we use $C_{\mathbf{h}_1} = 1/2$ and $C_{\mathbf{h}_2} = 1/(\sqrt{d} + 1)$ for our evaluation. For $\bar{A} = \max_k \mathbb{E}_q[|\dot{A}_k|^4]^{1/4}$, $\bar{B} = \max_k \mathbb{E}_q[|\dot{B}_k|^4]^{1/4}$, and $R = \bar{A}/(\bar{A} + \bar{B})$, clearly we have

$$\Gamma(\mathbf{h}_p; A, B) \leq (\bar{A} + \bar{B}) \left\{ R d \mathbb{E}_q[|h_p|^4]^{1/4} + (1 - R) \sum_{k=1}^d \mathbb{E}_q[|\partial_k h_p|^4]^{1/4} \right\}.$$

For $\mathbf{x} \sim N_d(\mathbf{1}_d \cdot 0.5, \mathbf{I}_d)$, we numerically evaluate $\mathbb{E}_q[|h_p|^4]$ and $\mathbb{E}_q[|\partial_k h_p|^4]$. Table 1 shows $\{R d \mathbb{E}_q[|h_p|^4]^{1/4} + (1 - R) \sum_{k=1}^d \mathbb{E}_q[|\partial_k h_p|^4]^{1/4}\}/C_{\mathbf{h}_p}$ of each dimension and weight for $R = 0.2, 0.8$.

In this problem setup, one can confirm that the upper bound for $p = 2$ is slightly smaller than that of $p = 1$ for all $R \in [0, 1]$, as the bound is the linear function of R . The theoretical conclusion verifies the numerical results.

H Increasing Boundary Size in Section 8.2

When experimenting with different values of L used in capping the distance function \bar{g}_L , an increasing boundary size (shown by values of b in Figure 5) is used in the experiments. The two regions, the square boundary and the disjoint boundary, are created by supplying set(s) of vertices Ω , detailing the locations of the polygonal truncation domain. The variable b

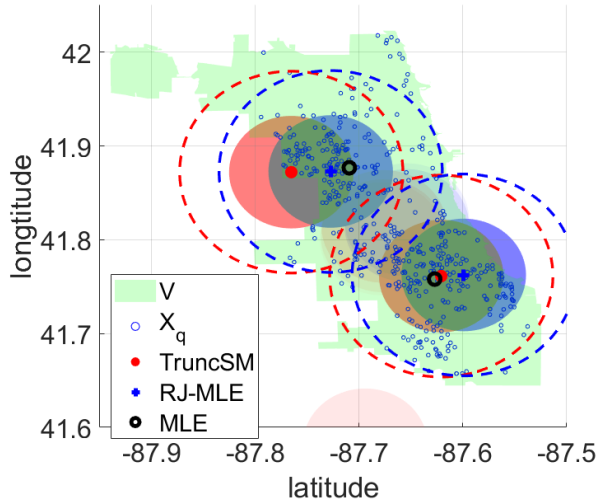


Figure 9: Chicago dataset: Gaussian mixture fitting with random initialization.

controls the boundary size by offsetting the supplied vertices in Ω . For the square, this was

$$\Omega_{\text{sq}} := \{(-b, -b), (-b, b), (b, b), (b, -b)\}.$$

Increasing b in this scenario leads to the corners of the square boundary being shifted by an equal amount. For the disjoint boundary, two sets of vertices were given for two disjoint domains:

$$\begin{aligned} \Omega_{\text{dis1}} &:= \{(1-b, 0.5-b), (1-b, 0.5), (1+b, 0.5), (1+b, 0.5-b)\}, \\ \Omega_{\text{dis2}} &:= \{(1-b, 1.5), (1-b, 1.5+b), (1+b, 1.5+b), (1+b, 1.5)\}. \end{aligned}$$

Increasing b in this case will enlarge the truncation domain while the “disjoint” section in the middle remains unchanged.

I Chicago Crime Dataset with Different Random Initialization

As we mentioned in Section 8.3, both TruncSM and RJ-MLE solve non-convex optimization problems so it is possible for them to return local optima. Therefore, to show the stability of both methods’ solutions, in this experiment, we randomly initialize both methods with the initial point $\boldsymbol{\mu}_q + \epsilon$, where $\boldsymbol{\mu}_q$ is the mean of the dataset X_q and $\epsilon \sim \mathcal{N}(\mathbf{0}, \mathbf{I}_d \cdot 0.06^2)$. Both methods were executed 500 times and each time, we plot two lightly shaded balls centered at the estimated mixture centers with their radius equal to the standard deviation. One can see from the blue/red shades in Figure 9, both algorithms consistently place centers at northern and southern Chicago, and both balls are roughly centered at locations reported in the Section 8.3. TruncSM also placed a Gaussian center outside of the boundary of Chicago in one of the simulations. This is a very rare event and such a result can be easily ruled out.